[American Journal of Science, Vol. 307, February, 2007, P. 339–370, DOI 10.2475/02.2007.02]

UPPER CAMBRIAN TO UPPER ORDOVICIAN PERI-GONDWANAN ISLAND ARC ACTIVITY IN THE VICTORIA LAKE SUPERGROUP, CENTRAL NEWFOUNDLAND: TECTONIC DEVELOPMENT OF THE NORTHERN GANDERIAN MARGIN

A. ZAGOREVSKI[*,§,†], C. R. VAN STAAL[*,**], V. MCNICOLL[**], and N. ROGERS[**]

ABSTRACT. The Exploits Subzone of the Newfoundland Appalachians comprises remnants of Cambro-Ordovician peri-Gondwanan arc and back-arc complexes that formed within the Iapetus Ocean. The Exploits Subzone experienced at least two accretionary events as a result of the rapid closure of the main portion of the Iapetus tract: the Penobscot orogeny (c. 480 Ma), which juxtaposed the Penobscot Arc (c. 513 – 486 Ma) with the Gander margin, and c. 450 Ma collision of the Victoria Arc (c. 473 – 454 Ma) with the Annieopsquotch Accretionary Tract that juxtaposed the peri-Laurentian and peri-Gondwanan elements along the Red Indian Line.

The newly recognized Pats Pond Group forms a temporal equivalent to other Lower Ordovician intra-oceanic complexes of the Penobscot Arc. The Pats Pond Group (c. 487 Ma) has a geochemical stratigraphy that is consistent with rifting of a volcanic arc. An ensialic setting is indicated by low εNd values (εNd 0.3 to -0.5) near the stratigraphic base and its abundant zircon inheritance (c. 560 Ma and 0.9 – 1.2 Ga). The spatial distribution of Tremadocian arc – back-arc complexes indicates that the Penobscot arc is best explained in terms of a single east-dipping subduction zone. This model is favored over west dipping models, in that it explains the distribution of the Penobscot arc elements, continental arc magmatism, and the obduction of back-arc Penobscot ophiolites without requiring subduction of the Gander margin or subduction reversal.

The newly recognized Wigwam Brook Group (c. 454 Ma) disconformably overlies the Pats Pond Group and records the youngest known phase of ensialic arc volcanism (εNd – 4.1) in the Victoria Arc, which is also related to east-dipping subduction. Thus the Penobscot and the overlying Victoria Arc are reinterpreted in terms of a single, relatively long-lived east-dipping subduction zone beneath the peri-Gondwanan microcontinent of Ganderia. The cessation of arc volcanism towards the top of the Wigwam Brook Group and the subsequent syn-tectonic sedimentation in the Badger Group constrain the arrival of the leading edge of Ganderia with the ensialic arc complexes to the Laurentian margin to c. 454 Ma.

INTRODUCTION

The Penobscot and Victoria arc systems of the Exploits Subzone formed during the complex Cambro-Ordovician closure of the Iapetus Ocean in proximity to Ganderia, a ribbon-like microcontinent outboard of Gondwana (van Staal and others, 1998). Following the Upper Ordovician arc-arc collision with the peri-Laurentian Red Indian Lake Arc, they were emplaced under the Annieopsquotch Accretionary Tract (for example, van Staal and others, 1998; van der Velden and others, 2004; Zagorevski and others, 2006) along the Red Indian Line (Williams, 1995) closing the main tract of Iapetus. This paper examines the latest stages of evolution of the Ordovician Victoria and Cambro-Ordovician Penobscot arcs. Two previously unrecognized volcano-sedimentary tectono-stratigraphic units are described, the Pats Pond and Wigwam Brook groups, based on detailed and regional mapping in central Newfoundland (Lissenberg and others, 2005; Rogers and others, 2005b; van Staal and others, 2005a,

*Ottawa-Carleton Geoscience Center, Department of Earth Sciences, University of Ottawa, 140 Louis Pasteur, Ottawa, Ontario, K1N 6N5, Canada
**Geological Survey of Canada, 601 Booth Street, Ottawa, Ontario, K1A OE8, Canada
§Present address: Geological Survey of Canada, 601 Booth Street, Ottawa, Ontario, K1A OE8, Canada
†Corresponding author email: azagorev@nrcan.gc.ca

2005b, 2005c) combined with geochronology and geochemistry. The identification of the position of the Red Indian Line based on the peri-Gondwanan affinity of the Pats Pond Group and Wigwam Brook Group and peri-Laurentian affinity of the adjacent Annieopsquotch Accretionary Tract (Zagorevski and others, 2006) requires revision of the north-western boundary of the peri-Gondwanan Victoria Lake supergroup (Evans and Kean, 2002), and enables an east-dipping subduction model to be developed for this portion of the Newfoundland Appalachians.

The Lower Ordovician Pats Pond Group was generated during the last stages of Penobscot Arc development. It is correlative to the previously defined lower Wild Bight, lower Exploits and lower Bay du Nord groups (O'Brien, 1992; Tucker and others, 1994; O'Brien and others, 1997; MacLachlan and Dunning, 1998) and places important constraints on the tectonic setting of the Tremadocian Penobscot Arc, including the polarity of subduction and involvement of peri-Gondwanan continental crust. The Upper Ordovician Wigwam Brook Group disconformably overlies the Pats Pond Group. The Wigwam Brook Group contains the youngest known arc volcanic rocks in the Victoria Arc and records the cessation of arc volcanism in the upper portions of its stratigraphy. The age and stratigraphic relationships in the Wigwam Brook Group place new time constraints on the Red Indian Lake – Victoria arc collision.

Regional Geology

The Dunnage Zone of the Newfoundland Appalachians contains the vestiges of the Cambro-Ordovician continental and intra-oceanic arc – back-arc and ophiolitic complexes that formed within the Iapetus Ocean (fig. 1; Williams, 1995). The Dunnage Zone is subdivided into the peri-Laurentian Notre Dame and Dashwoods subzones and the peri-Gondwanan Exploits Subzone (Williams, 1995). The peri-Laurentian and peri-Gondwanan subzones are differentiated on the basis of stratigraphic, structural, faunal and isotopic contrasts that are marked by the Red Indian Line, the fundamental suture zone of the Newfoundland Appalachians (fig. 1; Williams, 1995), which was subsequently imaged by Lithoprobe seismic reflection surveys as a major crustal scale fault (van der Velden and others, 2004).

To the west of the Red Indian Line, the peri-Laurentian Notre Dame Subzone is in part represented by the Annieopsquotch Accretionary Tract (fig. 1), a tectonic collage of arc and back-arc complexes that formed outboard of the Laurentian margin (van Staal and others, 1998; Zagorevski and others, 2006). To the east of the Red Indian Line, the peri-Gondwanan Exploits Subzone is dominated by volcanic and sedimentary rocks, which display a generally continuous Upper Ordovician-Silurian stratigraphy, contain lower-Ordovician insular (Celtic) faunas, and relatively radiogenic lead in mineral deposits (Williams, 1995). The Exploits Subzone of Newfoundland and its correlatives in New Brunswick have been interpreted to mainly represent the remnants of the Cambrian- Early Ordovician Penobscot and Early to Middle Ordovician Popelogan-Victoria arcs that formed outboard of the Gander margin (for example, van Staal, 1994; van Staal and others, 1998). The Penobscot arc has been generally considered to have developed in an intra-oceanic setting outboard of the Gander margin above a west-dipping subduction zone (for example, MacLachlan and Dunning, 1998a; van Staal and others, 1998), although the presence of continental basement has been inferred on the basis of Pb-isotope data (Swinden and Thorpe, 1984). The continued subduction culminated in the collision of the Penobscot arc and the Gander margin (van Staal and others, 1998), obduction of supra-subduction zone ophiolites on the Gander margin (Colman-Sadd and others, 1992; Jenner and Swinden, 1993) and subduction reversal (van Staal and others, 1998). The reversal resulted in subduction beneath the Ganderian margin and development of the younger Victoria arc above the Penobscot basement (for example, van Staal and others, 1998).

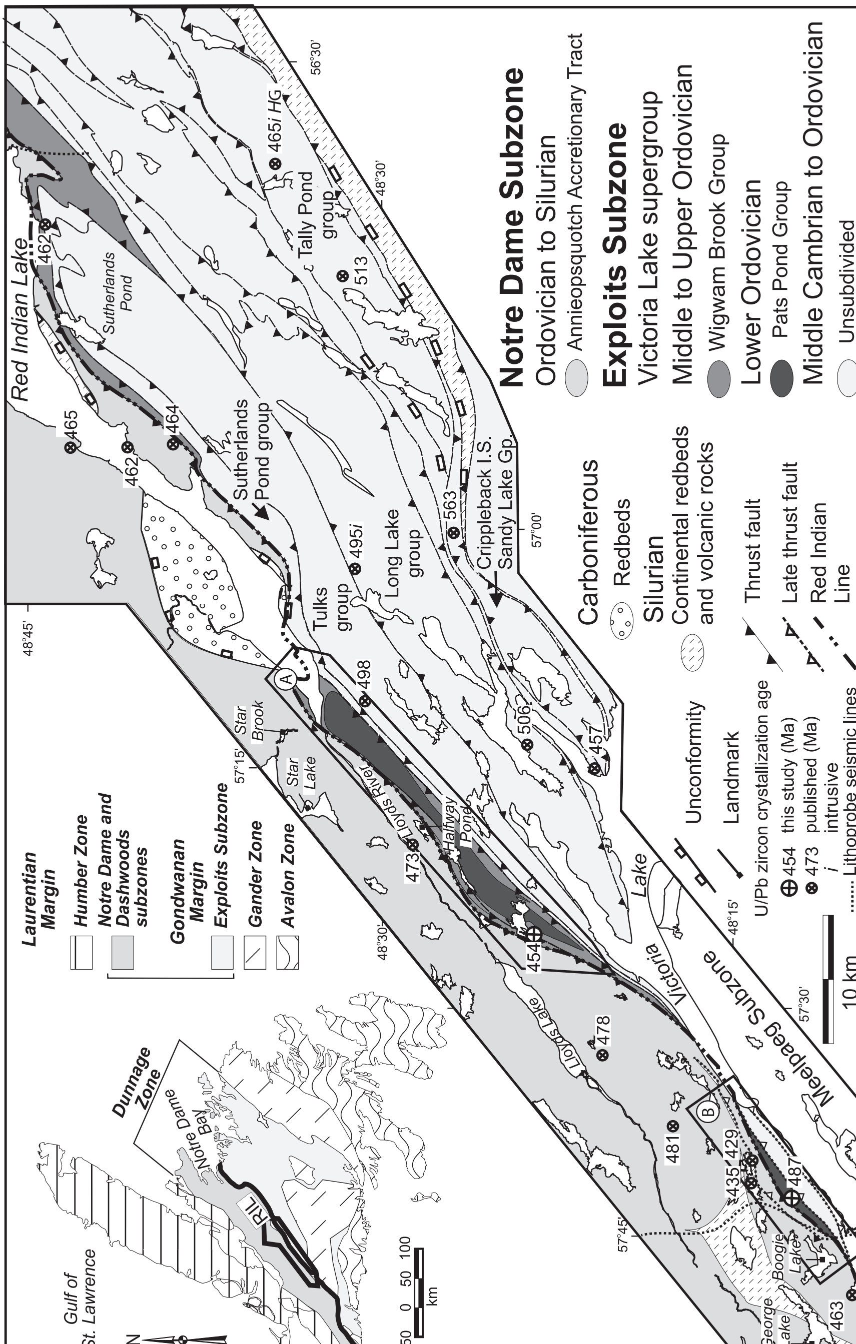

Fig. 1. Simplified geology of the study area (Lissenberg and others, 2005; Rogers and others, 2005b, 2006; van Staal and others, 2005a, 2005b, 2005c). Inset: Lithostratigraphic subdivisions of Newfoundland (after Williams, 1995). HG – Harpoon gabbro; I.S. - Igneous Suite; Gp. – Group.

Victoria Lake Supergroup

In central Newfoundland the tectonic elements of the Penobscot and Victoria arcs are represented by the Victoria Lake Group (Kean, 1977), which comprises Middle Ordovician and older volcanic and sedimentary rocks lying to the north of the Victoria Lake and southeast of the Red Indian Lake (fig. 1). The Victoria Lake Group is bound by the Red Indian Line to the west, Noel Pauls Line to the east and is overlain by (for example, Kean and Jayasinghe, 1980) or is in fault contact (for example, Rogers and others, 2005b) with Ordovician to Silurian sedimentary rocks of the Badger Group (Williams and others, 1995) to the northeast. Detailed investigations of the Victoria Lake Group required its informal elevation to supergroup status in order to reflect its composite nature (Evans and others, 1990; Evans and Kean, 2002; Rogers and van Staal, 2002). There have been several subdivisions of the Victoria Lake supergroup, the most recent one subdivides it into five distinct fault-bound belts with unique tectono-stratigraphy and age (fig. 1; Lissenberg and others, 2005; Rogers and others, 2005b; van Staal and others, 2005a, 2005b, 2005c). From east to west these include the Tally Pond Group (c. 513 Ma: Dunning and others, 1991), Long Lake group (c. 506 Ma: McNicoll and Rogers, unpublished data *in* van Staal and others, 2005c), Tulks group (c. 498 Ma: Evans and others, 1990), Sutherlands Pond group (c. 462 Ma: Dunning and others, 1987), Pats Pond and Wigwam Brook groups (c. 488 and c. 453 Ma respectively: *this study*; fig. 1).

STRATIGRAPHY

The rocks underlying the study area were previously included in the Tulks Hill volcanics (that is Tulks group: fig. 1) of the Victoria Lake supergroup (for example, Kean, 1977; Kean and Jayasinghe, 1981). However, recent mapping in association with detailed geochronology have required that the area be divided into several distinct tectono-stratigraphic units (Lissenberg and others, 2005; Rogers and others, 2005b; van Staal and others, 2005a, 2005b, 2005c), and that the stratigraphy be revised. Two new fault-bounded tectono-stratigraphic units are proposed herein, namely the Pats Pond and Wigwam Brook groups, which together form the western most portion of the Victoria Lake Supergroup (fig. 2).

The Pats Pond and Wigwam Brook groups form a shear zone-bound structural panel. They are metamorphosed to dominantly sub- to greenschist facies conditions and have experienced multiple phases of deformation from Middle Ordovician to Devonian. The macroscopic structural style in the study area is characterized by shear zone-truncated synform-antiform pairs. The shear zones are interpreted to represent mainly Middle Ordovician steepened southeast-directed thrust faults (D_1) which are marked by high strain phyllonites, mélange and broken formation (for example, Rogers and van Staal, 2002; Zagorevski, ms, 2006). The upright folding and steepening of thrusts occurred during the Late Ordovician to Middle Silurian Salinic orogeny (D_2) and was accompanied by transposition of D_1 fabrics. D_1 thrusts were commonly reactivated as Silurian south-southeast-directed reverse faults (Zagorevski, ms, 2006). Hence, the penetrative regional structures are a D_1 – D_2 composite. These are commonly overprinted by the Devonian northwest verging folds and shear zones (Zagorevski, ms, 2006) related to the emplacement of the Meelpaeeg subzone over the Exploits subzone (Valverde-Vaquero and others, 2006). The effects of multiple phases of folding, faulting, in association with possible thrust repetition and ubiquitous poor exposure, preclude any realistic estimations of the thickness of stratigraphic units.

The Pats Pond Group is exposed along Route 480 and in the Pats Pond area (figs. 1 and 2). In the Pats Pond – Red Indian Lake (fig. 2A) area the Lower Ordovician upward facing Pats Pond Group and disconformably overlying Upper Ordovician

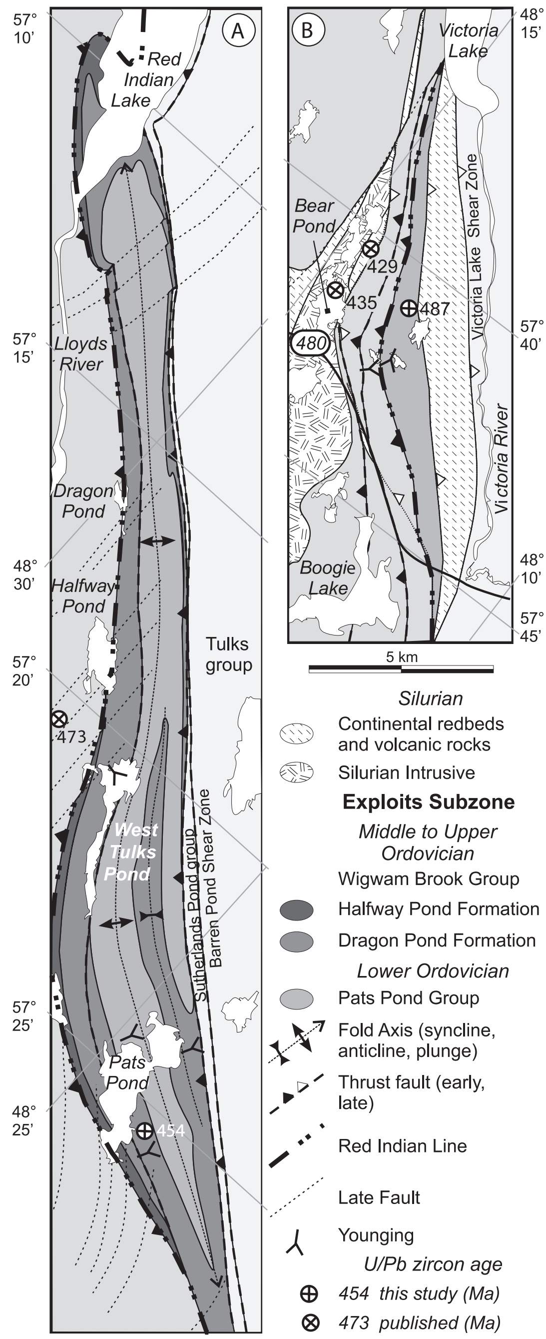

Fig. 2. Detailed geology of Pats Pond - Red Indian Lake area and Route 480 area.

Wigwam Brook Group are exposed in a doubly plunging anticline. The Wigwam Brook Group is bound to the northwest by the Red Indian Line, and to the southeast by the Barren Pond Shear Zone (fig. 2A). Near Route 480, the Pats Pond Group forms a southeast facing fault-bounded structural panel that is cut out to the southeast by the

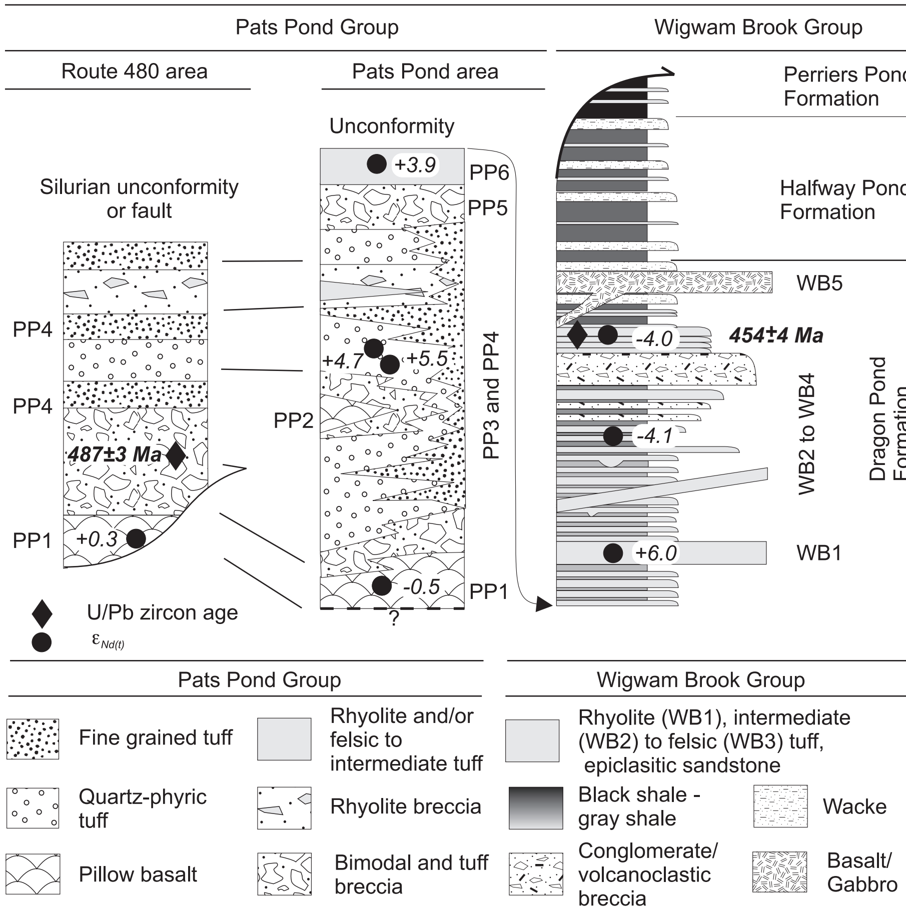

Fig. 3. Schematic stratigraphy of Lower Ordovician Pats Pond and upper Ordovician Wigwam Brook groups.

Victoria Lake Shear Zone (fig. 2B; Valverde-Vaquero and van Staal, 2002) and to the northwest by the Red Indian Line.

Pats Pond Group

The Pats Pond Group comprises mainly intertonguing mafic and intermediate tuffs. The discontinuous and interdigitating nature of these tuffs, combined with paucity of exposure and complex structure, precludes any formal subdivision of Pats Pond Group into formal geochemical members, however some informal geochemical types have been defined (PP1 to PP6: see *Geochemistry*, fig. 3). The sections in the Route 480 and Pats Pond areas were correlated on the basis of the lithological, geochemical and Sm-Nd isotopic characteristics of the volcanic rocks (fig. 3). Pillow basalt forms a distinct unit with limited exposure at the lowest exposed stratigraphic level of Pats Pond Group in the Route 480 area. The basalt is brown weathered and almost always sparsely to abundantly amygdaloidal. The amygdales are commonly radial with respect to the center of the pillow and are more abundant towards the top. Although the basalt appears aphyric in outcrop, most thin sections contain small to coarse euhedral colorless clinopyroxene phenocrysts and glomeroporhyrocrysts (fig. 4A) locally rimmed

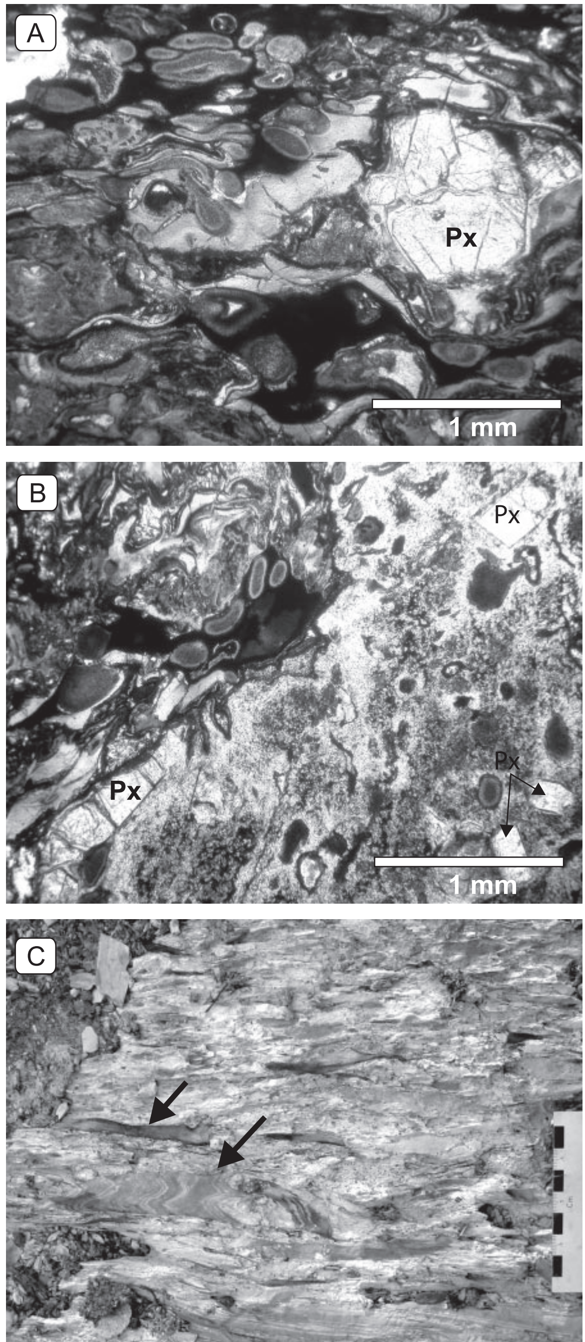

Fig. 4. Pats Pond Group bimodal tuff breccia unit; (A) pyroxene glomeroporphyritic mafic tuff matrix, (B) intermediate, pyroxene porphyritic lapilli in mafic tuff matrix (top left). (C) Tuff breccia unit at the dated locality of Wigwam Brook Formation containing accidental fragments of underlying epiclastic tuff, shale and dark shale (arrows), which are locally folded during subsequent deformation (scale in cm).

by colorless actinolite. Fragments of this basalt occur in the overlying tuff breccia in the Route 480 area.

Feldspar and/or quartz porphyritic ash tuff, lapilli tuff and tuff breccia are abundant and represent a characteristic unit of the Pats Pond Group. Breccia is commonly bimodal, and contains mafic and intermediate to felsic fragments in a finer-grained feldspar porphyritic mafic to intermediate groundmass. Feldspar comprises 5 to 45 percent of the rock by volume with crystal or glomeroporphyrocryst diameters ranging from <1 mm to >1 cm, although the average is around 3 to 4 mm. In general, quartz is subordinate and comprises less than 5 percent of the rock by volume, with crystal diameters from <1mm to 1 cm. Locally, both mafic and intermediate fragments contain small colorless microscopic phenocrysts of pyroxene (fig. 4B). Bimodal tuff grades into and is interlayered with light green to buff colored quartz (± feldspar) porphyritic andesitic tuff, lapilli tuff, tuff breccia, flows and related subvolcanic intrusions. Quartz phenocrysts may comprise as much as 40 percent by volume of the rock, with diameters ranging from 2 mm to 1 cm. Andesitic tuffs are overlain by bimodal mafic- aphyric felsic tuff breccia and aphyric rhyolite, which form the uppermost distinctive horizon in the Pats Pond Group. These rocks are in turn overlain by basaltic to andesitic tuff breccia, lapilli tuff and gray rhyolitic tuff, which form the highest observed stratigraphic horizon in the Pats Pond Group in the Pats Pond area (fig. 3).

Wigwam Brook Group

The Wigwam Brook is a volcano-sedimentary package of rocks exposed on the periphery of the doubly plunging anticline, which spans across Pats Pond to Red Indian Lake (fig. 2). Wigwam Brook Group continues further northeast as a fault bounded sliver (fig. 2). The contact with the Pats Pond Group is poorly exposed, but is interpreted to be an unconformity, because of the significant hiatus between the two groups (453 vs. 487 Ma: see following). The Wigwam Brook Group is subdivided into three lithologically distinct formations, namely the Dragon Pond, Halfway Pond, and Perriers Pond formations (fig. 3).

The Dragon Pond Formation dominantly comprises an overall coarsening-up sequence of felsic volcanic and volcaniclastic rocks. It has been informally subdivided into five geochemical types (WB1 to WB5: see *Geochemisty*, fig. 3). The base of the Dragon Pond Formation comprises a tuffaceous turbiditic sandstone and siltstone that is locally associated with dark shale, felsic tuff and tuff breccia, flow-banded rhyolite and felsic dikes. The tuffaceous turbidite is interlayered with and grades into a volcano-sedimentary breccia (fig. 4C) and conglomerate over a 20 m interval. The latter rocks have a predominantly local provenance, as is indicated by the abundance of angular clasts, similar to the underlying beds (fig. 4C). However, the presence of a few well-rounded granitoid cobbles suggests a minor contribution from a distal source. The breccia horizon is overlain by felsic tuff, lapilli tuff and tuff breccia containing fragments of turbidite and black shale. The uppermost portions of the Dragon Pond Formation contain gabbro sills, massive to pillowed basalt flows and mafic tuff.

The Halfway Pond Formation conformably overlies the Dragon Pond Formation and is mainly comprised of sedimentary rocks (fig. 3). The transition from the Dragon Pond Formation to the Halfway Pond Formation is gradational, and is marked by an increase in siltstone and shale and a decrease of the volcanic and epiclastic components. Unlike the Dragon Pond Formation where the sandstones are predominantly epiclastic, the wacke of the Halfway Pond Formation contains abundant smoky quartz and black shale fragments. A marked increase in abundance of black shale versus gray shale marks the transition from the Halfway Pond to the Perriers Pond Formation. The Perriers Pond Formation comprises abundant, locally calcareous, black shale with minor volcanogenic siltstone and sandstone and is most readily identifiable in the north-eastern portion of the mapped area, where it is commonly transformed into broken formation and mélange along the Red Indian Line. The Perriers Pond Formation generally has maximum structural thickness of only several hundred meters and is not plotted in figure 3, however it does form a mappable unit (for example, Rogers and others, 2005a, 2005b).

U-Pb GEOCHRONOLOGY

Analytical Techniques

SHRIMP II analyses were conducted at the Geological Survey of Canada (GSC) using analytical procedures described by Stern (1997), with standards and U-Pb calibration methods following Stern and Amelin (2003; see Appendix). Isoplot v. 2.49 (Ludwig, 2001) was used to generate concordia plots and calculate Concordia ages. The data are presented in table 1 and plotted in concordia diagrams with errors at the 2σ level (fig. 5).

Pats Pond Group VL01A-067 (z7252)

A sample of rusty weathering intermediate to bimodal breccia (VL01A-067) that overlies the lower calc-alkaline basalt was collected in the Route 480 area (figs. 1, 2, and 3). Based on the younging indicators, the dated bimodal breccia is one of the oldest rocks present in the Pats Pond Group in the Route 480 area (fig. 2B). The sample yielded sparse, fair quality zircon (n = 57). Angular fragments, with smaller amounts of prism fragments, prisms and rounded zircons, comprise the zircon population. Most of the zircons are euhedral and SEM study revealed oscillatory zoning in the majority of the zircon grains (n = 41), suggesting magmatic derivation. Some of these contained distinct, presumably inherited cores (n = 9). The rest of the grains (n = 16) were either not zoned or irregularly zoned and lacked crystal faces suggesting partial resorbtion. SHRIMP analysis yielded three distinct age populations of zircon: c. 487 Ma (n = 13), c. 553 Ma (n = 1), and c. 0.9 to 1.2 Ga (n = 5; fig. 5A, table 1). A Concordia age, calculated from the SHRIMP analyses of the youngest population, is 487 ± 3 Ma (MSWD of concordance and equivalence = 1.1, n = 12). All zircons in this population displayed oscillatory zoning (fig. 5A). This age of 487 ± 3 Ma is interpreted to represent the eruption age of the tuff breccia. Two analyses on a single un-zoned partially resorbed zircon are c. 553 Ma which is interpreted to be a xenocryst. The c. 0.9 to 1.2 Ga population is represented by slightly to moderately discordant xenocrystic zircons that were not zoned or irregularly zoned and partially resorbed.

Wigwam Brook Group VL01A-314 (z7630)

A sample of beige weathering, quartz and feldspar rich tuff (VL01A-314) immediately overlying the breccia-conglomerate horizon in the Dragon Pond Formation was collected in the Pats Pond area. The sample yielded abundant zircon with several distinct morphologies including: euhedral needles, prisms, equant multifaceted zircons; angular fragments; slightly to moderately rounded prisms; and very well rounded zircon grains. Most of the zircons were colorless to slightly yellow, however some of the very well rounded zircons were distinctly purple. SEM imaging of 87 zircons revealed mostly igneous oscillatory zoning and at least some euhedral faces on many zircons (fig. 5B). Some zircons contained distinct cores (n = 3). Several rounded zircons with irregular or no zoning (purple zircon) were also observed (n = 4). SHRIMP analyses have yielded two age populations of zircon. A Concordia age, calculated from the dominant age population, is 453 ± 4 Ma (MSWD of concordance and equivalence = 1.7, n = 22) (fig. 5B, table 1). This population includes both rounded and euhedral morphologies with oscillatory zoning, which showed no statistically significant difference in age (fig. 5B). This age of 453 ± 4 Ma is interpreted to represent the eruption

TABLE 1

U/Pb SHRIMP analytical data

Spot name	U (ppm)	Th (ppm)	Th/U	Pb* (ppm)	^{204}Pb (ppb)	$^{204}Pb/^{206}Pb$	$\pm\ ^{204}Pb/^{206}Pb$	$f(206)^{204}$	$^{208}Pb/^{206}Pb$	$\pm\ ^{208}Pb/^{206}Pb$	$^{207}Pb/^{235}U$	$\pm\ ^{207}Pb/^{235}U$	$^{206}Pb/^{238}U$	$\pm\ ^{206}Pb/^{238}U$	Corr Coeff	$^{207}Pb/^{206}Pb$	$\pm\ ^{207}Pb/^{206}Pb$	Ages (Ma)[1] $^{206}Pb/^{238}U$	Ages (Ma)[1] $\pm\ ^{206}Pb/^{238}U$	Ages (Ma)[1] $^{207}Pb/^{206}Pb$	Ages (Ma)[1] $\pm\ ^{207}Pb/^{206}Pb$	Ages (Ma)[2] $^{206}Pb/^{238}U$	Ages (Ma)[2] $\pm\ ^{206}Pb/^{238}U$
VLA01-067 (Z7252; UTM zone 21 449594 5341669, NAD83)																							
7252-18.1	116	64	0.569	9	3	0.000446	0.000117	0.0077	0.1846	0.0087	0.5962	0.0240	0.0766	0.0011	0.461	0.0565	0.0020	476	6	472	82	475	6
7252-25.1	157	79	0.519	13	3	0.000316	0.000114	0.0055	0.1562	0.0051	0.5936	0.0231	0.0768	0.0010	0.444	0.0561	0.0020	477	6	454	80	477	6
7252-2.1	91	44	0.494	7	2	0.000328	0.000155	0.0057	0.1477	0.0069	0.5672	0.0292	0.0772	0.0011	0.381	0.0533	0.0026	480	6	340	113	481	6
7252-54.1	101	50	0.509	8	4	0.000534	0.000232	0.0093	0.1650	0.0096	0.5960	0.0418	0.0773	0.0011	0.316	0.0559	0.0038	480	6	449	156	480	6
7252-43.1	135	76	0.581	11	3	0.000290	0.000107	0.0050	0.1811	0.0072	0.5902	0.0274	0.0787	0.0010	0.383	0.0544	0.0024	488	6	389	100	489	6
7252-49.1	106	32	0.315	8	3	0.000373	0.000160	0.0065	0.0969	0.0066	0.6288	0.0322	0.0788	0.0011	0.383	0.0579	0.0028	489	6	525	108	488	6
7252-26.1	187	120	0.661	16	2	0.000139	0.000066	0.0024	0.2145	0.0037	0.6358	0.0159	0.0789	0.0010	0.590	0.0584	0.0012	490	6	546	45	489	6
7252-23.1	120	49	0.421	10	3	0.000363	0.000123	0.0063	0.1365	0.0053	0.5843	0.0242	0.0790	0.0010	0.406	0.0537	0.0021	490	6	357	88	492	6
7252-48.1	214	142	0.686	19	2	0.000119	0.000059	0.0021	0.2188	0.0035	0.6244	0.0143	0.0790	0.0009	0.573	0.0573	0.0011	490	5	505	42	490	5
7252-37.1	122	68	0.576	10	3	0.000350	0.000136	0.0061	0.1801	0.0060	0.5974	0.0270	0.0790	0.0011	0.413	0.0548	0.0023	490	6	406	96	491	6
7252-6.1	119	69	0.595	10	0	0.000058	0.000111	0.0010	0.1914	0.0052	0.6283	0.0229	0.0792	0.0010	0.455	0.0575	0.0019	491	6	512	73	491	6
7252-27.1	130	68	0.540	11	2	0.000181	0.000118	0.0031	0.1782	0.0055	0.6410	0.0245	0.0799	0.0011	0.458	0.0582	0.0020	495	6	538	77	495	6
7252-52.1	256	211	0.851	24	2	0.000111	0.000050	0.0019	0.2730	0.0054	0.6509	0.0134	0.0810	0.0009	0.635	0.0583	0.0009	502	5	541	36	501	5
7252-57.2	195	16	0.085	16	1	0.000088	0.000073	0.0015	0.0295	0.0029	0.7244	0.0187	0.0885	0.0010	0.549	0.0593	0.0013	547	6	579	48	546	6
7252-57.1	269	22	0.084	23	2	0.000107	0.000102	0.0019	0.0277	0.0039	0.7321	0.0232	0.0905	0.0010	0.465	0.0587	0.0017	559	6	555	63	559	6
7252-56.1	100	134	1.382	21	4	0.000316	0.000085	0.0055	0.4326	0.0059	1.6157	0.0431	0.1613	0.0023	0.626	0.0726	0.0015	964	13	1004	43		
7252-42.1	45	15	0.356	8	4	0.000590	0.000172	0.0102	0.1054	0.0070	1.8379	0.0786	0.1763	0.0026	0.458	0.0756	0.0029	1047	14	1084	79		
7252-53.1	155	78	0.522	30	7	0.000272	0.000049	0.0047	0.1619	0.0026	1.9795	0.0383	0.1846	0.0024	0.747	0.0778	0.0010	1092	13	1141	26		
7252-55.1	40	20	0.515	8	0	0.000010	0.000010	0.0002	0.1817	0.0066	2.2457	0.0542	0.1926	0.0029	0.703	0.0846	0.0015	1135	15	1306	34		
7252-38.1	148	90	0.625	31	2	0.000093	0.000039	0.0016	0.1922	0.0025	2.1090	0.0355	0.1940	0.0023	0.790	0.0789	0.0008	1143	13	1169	21		
VLA01-314 (Z7630; UTM zone 21 468583 5360722, NAD83)																							
7630-22.1	322	123	0.396	23	7	0.000359	0.000197	0.0062	0.1151	0.0081	0.5194	0.0338	0.0701	0.0009	0.313	0.0537	0.0034	437	5	360	147	438	5
7630-30.1	185	117	0.653	14	2	0.000166	0.000177	0.0029	0.2063	0.0090	0.5606	0.0314	0.0712	0.0010	0.378	0.0571	0.0030	443	6	496	119	443	6
7630-19.1	169	135	0.822	14	0	0.000010	0.000010	0.0002	0.2580	0.0209	0.5876	0.0144	0.0717	0.0010	0.670	0.0595	0.0011	446	6	585	40	444	6
7630-7.1	325	185	0.588	25	4	0.000201	0.000236	0.0035	0.1903	0.0098	0.5325	0.0416	0.0718	0.0009	0.280	0.0538	0.0041	447	5	363	180	448	5
7630-56.1	248	137	0.570	19	4	0.000242	0.000205	0.0042	0.1694	0.0090	0.5514	0.0359	0.0719	0.0010	0.326	0.0556	0.0035	448	6	438	144	448	6
7630-6.1	405	103	0.263	29	0	0.000010	0.000010	0.0002	0.0855	0.0025	0.5589	0.0117	0.0722	0.0009	0.673	0.0561	0.0009	450	5	457	35	449	5
7630-9.1	245	132	0.557	19	1	0.000086	0.000135	0.0015	0.1724	0.0074	0.5294	0.0292	0.0723	0.0015	0.493	0.0531	0.0026	450	9	335	113	451	9
7630-55.1	556	522	0.970	47	0	0.000012	0.000060	0.0002	0.2946	0.0061	0.5646	0.0169	0.0724	0.0010	0.552	0.0566	0.0014	451	6	474	57	450	6
7630-5.1	236	149	0.653	19	0	0.000010	0.000010	0.0002	0.2100	0.0066	0.5853	0.0134	0.0726	0.0009	0.630	0.0585	0.0011	452	5	549	40	450	5
7630-20.1	95	54	0.590	7	1	0.000230	0.000529	0.0040	0.1985	0.0213	0.5662	0.0860	0.0726	0.0014	0.253	0.0566	0.0084	452	9	476	366	451	8
7630-46.1	103	54	0.545	8	3	0.000406	0.000544	0.0070	0.1846	0.0216	0.5560	0.0881	0.0726	0.0012	0.230	0.0556	0.0086	452	7	435	390	452	6
7630-12.1	376	240	0.660	29	3	0.000113	0.000111	0.0020	0.1973	0.0064	0.5615	0.0215	0.0727	0.0010	0.477	0.0560	0.0019	452	6	453	77	452	6
7630-50.1	649	457	0.728	52	0	0.000002	0.000053	0.0000	0.2204	0.0042	0.5575	0.0147	0.0728	0.0010	0.624	0.0555	0.0012	453	6	434	47	453	6
7630-11.1	168	152	0.930	14	0	0.000010	0.000010	0.0002	0.3037	0.0078	0.6057	0.0159	0.0729	0.0011	0.651	0.0603	0.0012	454	6	613	44	451	6
7630-40.1	274	255	0.961	24	1	0.000075	0.000196	0.0013	0.3133	0.0105	0.5666	0.0372	0.0729	0.0011	0.355	0.0564	0.0035	454	7	466	143	454	7
7630-41.1	523	300	0.592	41	0	0.000010	0.000010	0.0002	0.1919	0.0029	0.5721	0.0089	0.0731	0.0008	0.775	0.0567	0.0006	455	5	482	22	455	5
7630-48.1	230	98	0.443	17	4	0.000246	0.000298	0.0043	0.1397	0.0119	0.5516	0.0502	0.0735	0.0010	0.266	0.0544	0.0048	457	6	388	212	458	5
7630-18.1	377	227	0.620	30	4	0.000163	0.000060	0.0028	0.1871	0.0048	0.5493	0.0149	0.0741	0.0009	0.552	0.0538	0.0012	461	5	360	52	462	5
7630-64.1	198	145	0.754	16	0	0.000010	0.000010	0.0002	0.2287	0.0117	0.5800	0.0142	0.0747	0.0011	0.677	0.0563	0.0010	465	6	464	41	465	6
7630-17.1	94	53	0.584	7	3	0.000490	0.000301	0.0085	0.1682	0.0145	0.5340	0.0545	0.0748	0.0017	0.338	0.0518	0.0050	465	10	275	238	468	10
7630-2.1	119	107	0.927	10	2	0.000294	0.000473	0.0051	0.2940	0.0227	0.6235	0.0793	0.0750	0.0012	0.245	0.0603	0.0075	466	7	613	294	464	6
7630-49.1	221	106	0.496	17	2	0.000170	0.000098	0.0030	0.1493	0.0084	0.5743	0.0217	0.0752	0.0009	0.444	0.0554	0.0019	467	6	429	78	468	6
7630-3.1	106	73	0.707	61	0	0.000010	0.000010	0.0002	0.1856	0.0029	12.2733	0.1982	0.4829	0.0069	0.926	0.1843	0.0011	2540	30	2692	10		

Notes (see Stern, 1997): Uncertainties reported at 1σ (absolute) and are calculated by numerical propagation of all known sources of error. $f(206)^{204}$ refers to mole fraction of total ^{206}Pb that is due to common Pb, calculated using the ^{204}Pb-method; common Pb composition used is the surface bank. [1]204-corrected ages, [2]207-corrected ages (Stern, 1997)

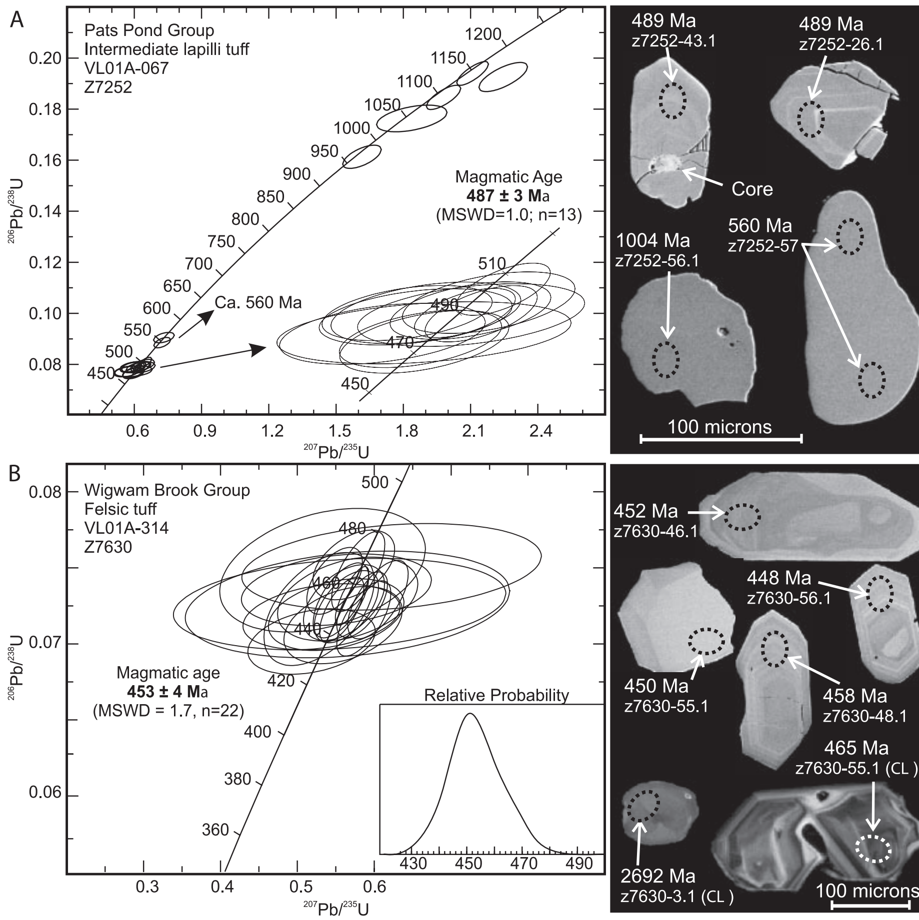

Fig. 5. U/Pb concordia diagrams and representative SEM images of zircons from the Pats Pond (A) and Wigwam Brook (B) groups. Circles represent the spot location. *CL* – cathode luminescence.

age of the tuff, although the presence of rounded zircons may suggest post-eruption reworking. One purple, un-zoned and rounded zircon was analyzed and yielded a discordant age of c. 2.7 Ga (table 1, not plotted).

GEOCHEMISTRY

The majority of the volcanic units have been sampled for geochemistry during this study and analyzed for major and trace elements using XRF and ICP-MS techniques (table 2). Samples are separated into groups based on stratigraphic position and chemical characteristics on extended spidergrams. Selected samples were analyzed for Sm-Nd isotopic composition (table 3; fig. 3). Complete analytical results, methods and errors are presented in Rogers (2004). Several ratios were calculated to facilitate the discussion of data, including La_n/Th_n, La_n/Nb_n, Zr_n/Sm_n, La_n/Sm_n and Gd_n/Lu_n (N-MORB normalization factors, Sun and McDonough, 1989). These ratios represent the intensity of the Th, Nb and Zr anomalies, and the slope of LREE and HREE. Cs, Rb, Ba, K, Pb and Sr are considered to be mobile (Cann, 1970) under the metamorphic and metasomatic conditions experienced by the rocks in this study. Only immobile elements are

TABLE 2

Geochemistry of peri-Gondwanan Penobscot and Victoria arc complexes

Sample	VL02A 026	VL02A 202	VL02A 204	VL02A 205	VL01A 341b	VL02A 150	VL01A 021	VL01A 067	VL01A 344	VL02A 121
UTMx[†]	448003	484514	484361	484179	469183	470046	453123	449594	470315	477638
UTMy[†]	5341400	5376241	5376134	5375787	5360797	5362877	5344015	5341669	5360839	5367582
NTS map	12A/04	12A/11	12A/11	12A/11	12A/06	12A/06	12A/04	12A/04	12A/06	12A/06
Type	PP_1	PP_1	PP_1	PP_1	PP_2	PP_2	PP_3	PP_3	PP_3	PP_3
Rock type[‡]	pbslt	pbslt	bslt	bslt	mtuff (fp)	mtuff	ituff (fqp)	ituff (fp)	ituff (fp)	ituff (fqp)
Laboratory[§]	1	1	1	1	2	1	2	2	3	1
SiO_2 (wt%)	46.65	50.39	56.02	50.66	48.36	46.48	59.50	49.41	67.79	54.26
TiO_2	0.75	0.64	0.73	0.70	0.38	0.39	0.32	0.59	0.44	0.35
Al_2O_3	16.29	15.37	14.18	15.19	16.17	18.11	15.46	18.80	13.05	17.16
MnO	0.12	0.16	0.16	0.19	0.09	0.20	0.12	0.16	0.03	0.15
MgO	9.59	8.88	6.00	9.40	8.26	6.97	3.02	5.44	1.81	5.51
CaO	8.57	7.46	6.09	5.32	9.86	11.83	6.23	8.57	6.90	6.59
Na_2O	3.10	4.21	5.93	4.97	1.34	0.83	2.11	1.38	2.92	3.67
K_2O	0.99	0.09	0.22	0.05	0.13	0.02	2.47	0.01	0.02	0.68
P_2O_5	0.13	0.10	0.11	0.15	0.02	0.05	0.04	0.04	0.24	0.03
LOI	5.05	3.06	1.58	3.58	4.39	3.79	5.56	3.94	2.20	2.50
Fe_2O_3 total	8.73	9.75	9.21	9.89	12.20	11.62	5.95	12.88	4.48	9.48
Total	100.07	100.20	100.27	100.23	101.21	100.33	100.78	101.22	99.89	100.41
Ba (ppm)	72	49	129	23	96	12	146	11	39	647
Cr	388	420	82	582	56	96	57	59	27	35
Cs	0.86	0.15	0.28	0.14	0.08	0.08	1.84	0.08	b.d.	0.44
Hf	1.30	1.00	1.20	1.20	0.40	0.40	1.10	0.90	1.40	1.00
Nb	1.48	0.63	0.86	1.00	0.58	0.53	0.74	0.55	1.40	0.90
Ni	144	135.3	31.2	174	25.0	31.6	16.9	16.9	4.40	12.5
Pb	2.20	2.20	1.80	3.30	6.20	6.40	3.60	5.91	9.50	2.30
Rb	18.45	0.64	2.56	0.45	2.13	0.14	57.7	b.d.	b.d.	12.0
Sc	39.0	44.3	41.7	52.5	48.5	48.8	31.7	49.1	16.0	36.7
Sr	284	157	119	234	223	323	119	367	197	177
Ta	0.22	0.16	0.17	0.18	b.d.	0.15	b.d.	b.d.	b.d.	0.18
Th	1.82	1.72	2.12	4.06	0.93	0.92	0.98	0.87	1.80	0.68
U	0.57	0.46	0.50	1.01	0.43	0.72	0.44	0.52	1.20	0.31
V	256	315	315	315	315	315	190	351	53.0	210
Y	19.14	15.56	19.05	18.21	5.22	6.14	15.05	12.26	29.70	15.29
Zr	44.40	30.20	43.20	44.40	13.05	12.90	34.64	27.02	42.70	29.70
La	8.33	5.80	7.50	11.18	3.38	3.34	2.85	3.01	8.10	2.97
Ce	19.43	13.32	17.80	25.28	7.23	7.03	6.80	7.66	16.40	6.83
Pr	2.63	1.85	2.41	3.37	0.92	0.88	0.92	1.13	2.15	0.99
Nd	12.22	8.33	10.75	14.49	3.82	3.58	4.48	5.40	10.80	4.76
Sm	3.02	2.23	2.92	3.64	0.92	0.89	1.34	1.62	2.20	1.54
Eu	1.00	0.71	0.88	0.97	0.38	0.32	0.46	0.84	0.87	0.54
Gd	3.18	2.43	2.84	3.50	0.94	0.95	1.84	1.86	3.68	1.86
Tb	0.56	0.44	0.51	0.57	0.16	0.16	0.34	0.34	0.64	0.37
Dy	3.19	2.57	3.21	3.17	0.99	1.00	2.23	2.19	4.16	2.20
Ho	0.71	0.57	0.65	0.69	0.22	0.23	0.50	0.51	1.02	0.56
Er	2.12	1.57	1.95	2.05	0.59	0.69	1.55	1.39	2.82	1.70
Tm	0.31	0.24	0.31	0.29	0.10	0.12	0.24	0.20	0.52	0.29
Yb	1.98	1.75	1.90	1.75	0.61	0.73	1.60	1.30	3.21	1.59
Lu	0.31	0.23	0.28	0.28	0.10	0.12	0.28	0.23	0.47	0.30
Mg#[††]	70.5	66.5	58.7	67.4	59.6	56.7	52.5	47.9	46.8	55.9
(La/Th)n[‡‡]	0.2	0.2	0.2	0.1	0.2	0.2	0.1	0.2	0.2	0.2
(La/Nb)n	5.2	8.6	8.1	10.4	5.4	5.9	3.6	5.1	5.4	3.1
(Zr/Sm)n	0.52	0.48	0.53	0.43	0.5	0.52	0.92	0.59	0.69	0.69
(La/Sm)n	2.9	2.74	2.7	3.23	3.86	3.95	2.24	1.95	3.87	2.03
(Gd/Lu)n	1.27	1.31	1.25	1.55	1.16	0.98	0.81	1	0.97	0.77

plotted on the extended trace element spidergrams presented in figure 6 (N-MORB normalized; Sun and McDonough, 1989). FeO and Mg# were calculated assuming a Fe^{3+}/Fe^{2+} ratio of 0.1. Tectonic discrimination of felsic volcanic rocks is aided by Yb – Ta plot of Pearce and others (1984) as the more commonly used plot, Rb – (Y+Nb), may be affected by the mobility of Rb. Both Yb – Ta and Rb – (Y+Nb) plots require "fresh, non-porphyry, non-cumulate, non-aplitic intrusive rocks containing visible free quartz . . . > 5 modal %" (Pearce and others, 1984). When the Rb – (Y+Nb) diagram was subsequently evaluated on a broader dataset of granitic rocks which, included "felsic rocks containing modal quartz but not necessarily K-feldspar, and with SiO_2 contents greater than 60%" (Foerster and

TABLE 2

(continued)

Sample	VL02A 134b	VL01A 335	VL01A 336	VL02A 128	VL02A 135	VL02A 199	VL02A 200b	VL02A 221	VL02A 104	VL02A 122a
UTMx[†]	475491	470759	470187	473877	475697	480957	483707	486013	468948	477869
UTMy[†]	5366640	5361846	5361777	5365750	5366577	5371665	5373650	5375420	5358950	5367612
NTS map	12A/06	12A/06	12A/06	12A/06	12A/06	12A/06	12A/11	12A/11	12A/06	12A/06
Type	PP_3	PP_4	PP_4	PP_4	PP_4	PP_4	PP_4	PP_4	PP_5	PP_6
Rock type[‡]	ituff (fqp)	ftuff (qfp)	ftuff	ftuff	ftuff	ftuff (qp)	ftuff (qp)	ftuff (qfp)	ituff	ftuff
Laboratory[§]	1	4	2	1	1	3	1	1	1	1
SiO_2 (wt%)	61.15	64.00	72.69	65.63	65.54	61.46	67.81	67.83	49.26	83.46
TiO_2	0.30	0.32	0.26	0.29	0.24	0.29	0.24	0.30	0.81	0.13
Al_2O_3	14.59	14.40	12.89	13.42	13.92	14.68	14.19	12.34	18.59	9.40
MnO	0.09	0.10	0.02	0.10	0.09	0.11	0.03	0.08	0.12	0.01
MgO	3.59	3.00	1.70	2.25	2.12	4.11	2.65	3.02	5.46	0.26
CaO	5.94	1.46	1.90	6.19	6.17	3.02	3.17	4.19	5.43	0.23
Na_2O	2.61	5.25	5.26	3.06	3.31	2.47	3.26	2.10	3.93	5.36
K_2O	0.04	0.17	0.30	0.63	0.12	1.62	0.61	0.34	1.46	0.03
P_2O_5	0.06	0.05	0.06	0.07	0.05	0.03	0.05	0.04	0.02	0.02
LOI	3.04	7.01	1.35	2.15	2.25	3.40	2.30	2.32	5.80	0.24
Fe_2O_3 total	8.68	8.00	3.85	6.17	6.35	8.72	5.58	7.44	9.04	0.75
Total	100.11	99.80	100.29	99.98	100.18	99.95	99.90	100.02	99.95	99.90
Ba (ppm)	24	102	25	43	11	259	48	53	81	13
Cr	38	23	0.5	35	35	21	21	41	31	17
Cs	0.11	0.10	0.08	0.19	0.12	0.30	0.21	0.21	0.69	0.08
Hf	1.30	1.50	1.42	0.70	0.80	1.40	1.50	1.20	1.10	3.40
Nb	1.04	1.20	0.92	0.50	0.51	1.00	0.93	0.92	0.97	3.46
Ni	10.4	5.00	b.d.	11.7	9.52	7.00	5.10	12.1	13.0	2.96
Pb	4.30	2.00	2.96	4.10	4.00	3.30	6.00	7.20	1.40	3.00
Rb	0.40	2.70	3.34	6.06	1.86	13.2	4.38	4.54	17.8	0.24
Sc	38.8	31.0	20.6	37.1	37.3	33.0	27.0	35.2	32.1	7.50
Sr	76	87	70	143	156	177	101	85.1	151	32.3
Ta	0.18	b.d.	b.d.	0.16	0.17	b.d.	0.17	0.20	0.19	0.26
Th	1.47	1.80	1.11	0.51	0.61	2.20	1.17	1.28	0.39	4.18
U	0.59	0.62	0.60	0.57	0.35	1.00	0.66	0.96	0.16	1.22
V	214	136	58.3	199	184	220	88.8	232	315	3.8
Y	18.97	20.00	22.96	16.22	20.65	16.60	30.12	12.75	16.5	35.0
Zr	44.90	52.00	45.42	21.90	27.30	37.80	46.60	38.00	35.9	111
La	4.22	5.20	4.15	2.26	3.63	4.30	4.35	3.33	1.86	8.80
Ce	9.46	11.00	9.10	5.26	8.29	9.40	10.04	8.04	4.96	19.88
Pr	1.25	1.40	1.26	0.70	1.08	1.07	1.39	1.07	0.75	2.46
Nd	5.61	6.60	5.78	3.32	5.14	5.10	7.07	4.71	4.28	10.37
Sm	1.70	1.80	1.90	1.23	1.55	2.10	2.19	1.39	1.43	2.76
Eu	0.40	0.40	0.62	0.39	0.40	0.38	0.53	0.32	0.61	0.48
Gd	2.22	2.40	2.62	1.58	2.35	2.17	3.19	1.50	2.14	3.75
Tb	0.44	0.43	0.51	0.32	0.46	0.36	0.60	0.34	0.42	0.72
Dy	2.84	2.90	3.48	2.23	2.99	2.21	4.39	2.03	2.82	5.18
Ho	0.69	0.67	0.86	0.54	0.69	0.54	1.07	0.46	0.60	1.18
Er	2.10	2.10	2.55	1.79	2.15	1.70	3.33	1.48	1.85	3.97
Tm	0.35	0.35	0.43	0.32	0.37	0.29	0.56	0.24	0.30	0.61
Yb	2.16	2.40	2.86	1.88	2.21	1.98	4.03	1.55	2.00	4.29
Lu	0.38	0.42	0.49	0.33	0.37	0.37	0.68	0.26	0.31	0.71
Mg#[††]	47.4	45	49	44.3	42.1	50.7	50.9	46.9	56.8	43
(La/Th)n[‡‡]	0.1	0.1	0.2	0.2	0.3	0.1	0.2	0.1	0.2	0.1
(La/Nb)n	3.8	4	4.2	4.2	6.6	4	4.4	3.4	1.8	2.4
(Zr/Sm)n	0.94	1.03	0.85	0.63	0.63	0.64	0.76	0.97	0.89	1.43
(La/Sm)n	2.61	3.04	2.3	1.93	2.46	2.15	2.09	2.52	1.37	3.35
(Gd/Lu)n	0.72	0.71	0.66	0.59	0.79	0.73	0.58	0.71	0.85	0.65

others, 1997) no significant difference was found between the plutonic and volcanic rocks in their study. Since volcanic rocks essentially represent liquidus magmatic compositions and no significant differences were identified in related plots, we infer that the Yb – Ta plot can be utilized in this study as a preliminary discriminant of the tectonic setting of felsic volcanic rocks.

Pats Pond Group

Pats Pond Group comprises six informal geochemical types that occur at distinct stratigraphic levels. In ascending order, they are informally referred herein as PP_1-PP_6, such that type PP_1 comprises the lowest exposed stratigraphic unit and type PP_6 occurs

TABLE 2
(continued)

Sample	VL02A 246b	VL02A 140b	VL02A 186	VL01A 347	VL02A 218b	VL02A 262b	RAX01 034	RAX01 082	RAX01 914	RAX02 117
UTMx[†]	478760	475721	471462	468280	485985	486138	506207	505319	523396	527100
UTMy[†]	5368443	5367161	5365230	5360643	5377340	5377671	5387828	5387227	5399306	5395447
NTS map	12A/06	12A/06	12A/06	12A/06	12A/11	12A/11	12A/10	12A/10	12A/10	12A/10
Type	PP_6 ftuff	WB_1	WB_1	WB_2	WB_2	WB_2	WB_3	WB_3	WB_3	WB_3
Rock type[‡]	(qp)	rhyolite	rhyolite	rhyolite	ftuff	ftuff	atuff	ftuff	ftuff	ftuff
Laboratory[§]	1	3	1	3	1	1	5	5	5	3
SiO_2 (wt%)	79.89	84.41	76.23	63.73	61.48	60.24	58.48	67.52	74.33	75.90
TiO_2	0.19	0.12	0.06	0.74	0.57	0.74	0.59	0.42	0.22	0.33
Al_2O_3	11.47	8.24	12.82	14.47	18.00	17.14	18.44	16.43	13.79	11.63
MnO	0.01	0.01	0.02	0.12	0.10	0.06	0.18	0.18	0.09	0.11
MgO	0.31	0.10	1.97	2.80	2.86	2.06	1.68	1.68	2.01	0.19
CaO	0.09	0.65	0.41	2.46	2.19	3.55	5.17	0.28	0.66	0.20
Na_2O	6.09	3.79	1.13	3.64	4.45	3.42	3.42	3.83	4.76	3.05
K_2O	0.33	0.53	3.26	1.29	1.79	2.93	2.85	2.81	1.80	1.34
P_2O_5	0.04	0.03	0.01	0.60	0.18	0.23	0.27	0.06	0.07	0.05
LOI	0.42	1.00	2.42	2.40	2.67	4.83	3.55	2.55	1.72	2.00
Fe_2O_3 total	1.30	0.96	1.50	7.57	5.92	5.25	6.28	5.07	2.14	3.87
Total	100.15	99.89	99.84	99.85	100.21	100.46	100.89	101.07	99.76	99.84
Ba (ppm)	70	476	168	216	248	354	539	617	396	281
Cr	14	7	13	7	9	21	3	15	b.d.	55
Cs	0.13	0.10	2.45	0.60	1.79	1.89	1.88	2.24	1.13	2.00
Hf	3.60	3.00	10.90	4.00	4.80	3.90	2.94	3.58	2.25	2.30
Nb	3.79	8.50	147.30	7.40	3.36	2.68	2.66	8.68	7.41	4.50
Ni	3.00	2.60	3.34	13.1	1.72	8.33	b.d.	8.61	b.d	16.4
Pb	1.90	4.40	12.90	8.10	4.30	2.40	2.41	18.68	4.54	4.80
Rb	4.07	10.3	85.3	30.4	45.8	73.4	75.2	88.5	58.9	44.4
Sc	10.4	2.00	1.55	21.0	16.8	22.1	10.9	18.5	3.96	9.00
Sr	34.9	96.5	71.3	247	258	168	436	49.0	152	89
Ta	0.37	0.60	6.36	0.40	0.30	0.28	b.d.	0.53	0.61	0.30
Th	3.50	2.00	15.36	4.30	8.30	6.72	8.05	9.17	5.93	6.30
U	1.11	0.50	4.91	2.60	2.72	1.81	2.30	2.07	1.02	1.00
V	10.1	9.0	3.6	85.0	18.7	66.3	88.3	70.6	22.0	66.0
Y	55.3	29.4	85.3	65.5	45.3	45.5	22.9	25.2	10.6	12.2
Zr	122	78.3	209	124	173	142	96.7	111	76.4	74.9
La	9.08	7.50	21.26	37.20	21.32	20.77	27.98	24.34	18.09	19.30
Ce	22.26	14.30	54.42	78.90	50.28	48.16	56.88	48.08	34.19	33.10
Pr	2.91	1.91	7.63	8.61	7.34	6.57	7.31	5.79	4.02	3.65
Nd	13.10	8.30	31.41	38.50	32.55	29.81	28.55	21.26	13.65	14.90
Sm	3.23	2.10	10.93	8.20	7.14	7.12	5.56	4.36	2.56	2.60
Eu	0.61	1.19	0.04	2.05	2.23	1.99	1.75	1.01	0.52	0.66
Gd	4.87	3.48	12.80	8.70	6.60	7.23	4.90	4.24	1.96	2.01
Tb	1.03	0.61	2.56	1.39	1.22	1.19	0.71	0.72	0.32	0.33
Dy	7.24	4.12	16.11	9.14	7.61	7.58	4.08	4.38	1.86	2.28
Ho	1.76	0.85	3.27	2.03	1.64	1.57	0.86	0.94	0.35	0.41
Er	5.71	2.80	10.02	5.51	4.99	4.82	2.36	2.78	1.02	1.39
Tm	0.86	0.44	1.70	0.99	0.80	0.78	0.37	0.43	0.15	0.21
Yb	5.59	2.91	11.72	5.67	5.10	4.77	2.50	2.89	1.07	1.56
Lu	0.91	0.39	1.95	0.93	0.84	0.79	0.42	0.46	0.17	0.30
Mg#[††]	34.2	18.5	74.1	44.6	51.3	46.1	36.8	46.4	16.2	43.9
(La/Th)n[‡‡]	0.1	0.2	0.1	0.4	0.1	0.1	0.2	0.1	0.1	0.1
(La/Nb)n	2.2	0.8	0.1	4.7	5.9	7.2	9.8	2.6	2.3	4
(Zr/Sm)n	1.34	1.33	0.68	0.54	0.86	0.71	0.62	0.9	1.06	1.02
(La/Sm)n	2.96	3.76	2.05	4.77	3.14	3.07	5.29	5.87	7.43	7.81
(Gd/Lu)n	0.66	1.1	0.81	1.16	0.97	1.13	1.44	1.14	1.43	0.83

near the stratigraphic top. PP_1 (n = 4) consists of transitional calc-alkaline basaltic andesite to island arc tholeiite (figs. 6 and 7A). The samples exhibit consistently strong Th enrichment (average La_n/Th_n 0.2), strong Nb depletion (La_n/Nb_n 8.1), slight Ti depletion, negative Zr and Hf anomalies (Zr_n/Sm_n 0.5), strong enrichment of LREE (La_n/Sm_n 2.9) and slight enrichment of MREE (Gd_n/Lu_n 1.4). The samples are primitive to moderately evolved (Mg# 70.5 to 58.7). Sm-Nd isotopic analyses of two samples yielded εNd_{487} values of -0.54 and +0.34 (table 3).

PP_2 (n = 2) comprises calc-alkaline basalt and mafic tuff and is locally intercalated with $PP_{3\text{-}4}$ andesite (figs. 6 and 7A). The samples have very similar trace element profiles to PP_1 on extended spidergrams, however, they have overall lower absolute

TABLE 2

(continued)

Sample	VL01A 325	VL01A 327b	VL02A 209b	RAX02 123	RAX02 124	RAX01 008	RAX01 053	VL01A 326a	VL02A 093	VL02A 137b
UTMx†	467791	468324	485544	541568	540962	507160	486738	468783	468913	475442
UTMy†	5359382	5361335	5378179	5408696	5408352	5388689	5378303	5361759	5363345	5367675
NTS map	12A/06	12A/06	12A/11	12A/16	12A/16	12A/10	12A/11	12A/06	12A/06	12A/06
Type	WB_3	WB_3	WB_3	WB_4	WB_4	WB_5	WB_5	WB_5	WB_5	WB_5
Rock type‡	ftuff	rhyolite	ftuff	ftuff	ftuff	pbslt	pbslt	gabbro	bslt	bslt
Laboratory§	3	2	1	6	6	5	5	4	1	1
SiO_2 (wt%)	69.67	73.11	72.24	69.45	67.58	45.86	47.51	48.30	47.26	50.80
TiO_2	0.46	0.40	0.35	0.40	0.46	0.71	0.57	0.95	1.29	1.99
Al_2O_3	12.90	10.72	14.17	13.49	13.35	17.28	11.02	15.10	15.95	14.01
MnO	0.07	0.21	0.14	0.15	0.18	0.12	0.16	0.17	0.17	0.20
MgO	2.29	1.94	0.96	1.31	2.22	6.48	7.33	8.61	7.90	5.51
CaO	1.79	0.83	0.93	2.59	1.76	6.96	12.63	7.39	8.72	7.82
Na_2O	2.78	3.32	4.44	2.77	4.19	1.12	4.73	3.41	3.87	4.53
K_2O	1.93	0.35	2.10	2.20	1.06	2.87	0.78	0.28	0.25	0.24
P_2O_5	0.09	0.07	0.10	0.10	0.13	0.12	0.08	0.07	0.12	0.17
LOI	2.80	2.12	1.69	2.30	2.39	9.28	9.26	6.24	3.62	1.83
Fe_2O_3 total	4.99	7.18	3.09	5.80	6.80	9.72	6.59	12.00	11.37	13.11
Total	99.84	100.26	100.22	100.57	100.13	100.53	100.65	99.10	100.61	100.25
Ba (ppm)	481	113	798	589	542	227	160	44	58	31
Cr	55	41	32	29	20	252	338	199	316	32
Cs	1.40	0.30	2.88	2.24	1.64	2.83	3.18	0.19	0.17	1.22
Hf	2.20	2.36	3.20	1.70	1.40	1.34	1.05	1.30	1.90	3.40
Nb	6.00	8.15	7.19	1.08	1.08	0.82	0.68	0.67	1.09	1.22
Ni	25.1	23.4	7.66	3.37	2.99	90.1	153	73.0	118	24.2
Pb	18.40	26.41	9.60	10.10	15.00	2.12	1.31	b.d.	1.70	2.60
Rb	61.8	11.8	79.7	39.6	25.2	53.8	21.3	3.40	3.13	9.23
Sc	14.0	9.49	12.5	27.1	28.9	35.2	28.2	45.0	52.5	41.2
Sr	180	178	183	191	534	145	224	115	120	155
Ta	0.40	0.49	0.60	0.16	0.18	0.15	0.15	b.d.	0.22	0.22
Th	6.80	7.11	10.05	2.63	1.96	1.46	1.17	0.52	0.53	0.86
U	1.70	1.46	2.43	1.44	1.00	1.04	0.47	0.14	0.55	0.22
V	100	50.2	68.4	71.0	83.4	312	225	344	360	424
Y	21.9	15.6	21.8	23.2	24.0	17.7	12.1	29.0	28.1	51.0
Zr	92.3	83.8	131	53.1	41.6	43.1	33.8	42.0	71.8	119
La	23.10	22.92	38.66	7.25	6.52	5.31	5.02	3.30	5.18	5.50
Ce	43.70	58.15	53.89	15.46	13.78	12.87	12.11	8.50	10.85	15.29
Pr	5.28	5.53	8.00	1.97	1.80	1.86	1.78	1.30	1.88	2.56
Nd	22.20	20.08	28.96	8.78	7.98	8.57	7.99	7.30	9.62	14.34
Sm	4.10	3.81	5.10	2.51	2.23	2.46	2.02	2.30	3.03	4.96
Eu	0.84	0.84	1.25	0.63	0.68	0.91	0.78	0.74	1.14	1.82
Gd	3.16	3.16	4.23	3.08	3.02	2.81	2.19	3.30	4.21	6.90
Tb	0.58	0.51	0.59	0.56	0.56	0.46	0.36	0.66	0.72	1.30
Dy	3.78	2.92	3.71	3.58	3.78	3.11	2.24	4.30	4.47	8.07
Ho	0.71	0.61	0.73	0.85	0.88	0.71	0.48	0.94	1.00	1.92
Er	2.12	1.65	2.27	2.63	2.61	2.12	1.40	2.60	3.01	5.42
Tm	0.33	0.26	0.35	0.42	0.44	0.31	0.23	0.43	0.42	0.86
Yb	2.19	1.62	2.44	2.69	2.79	2.18	1.25	2.80	2.76	5.12
Lu	0.37	0.26	0.34	0.45	0.46	0.33	0.21	0.44	0.39	0.83
Mg#††	50	37.1	40.4	33	41.6	59.2	70.8	61	60.2	47.8
(La/Th)n‡‡	0.2	0.2	0.2	0.1	0.2	0.2	0.2	0.3	0.5	0.3
(La/Nb)n	3.6	2.6	5	6.3	5.6	6	6.9	4.6	4.4	4.2
(Zr/Sm)n	0.8	0.78	0.91	0.75	0.66	0.62	0.59	0.65	0.84	0.85
(La/Sm)n	5.93	6.33	7.97	3.04	3.08	2.27	2.61	1.51	1.8	1.17
(Gd/Lu)n	1.06	1.5	1.54	0.85	0.81	1.05	1.29	0.93	1.33	1.03

†UTM zone 21 (NAD83); ‡ (p)bslt-(pillowed)basalt; (s)diab-(sheeted)diabase; gabb-gabbro; (f, i, m)tuff-(felsic, intermediate, mafic) tuff; gran-granodiorite; rhyo-rhyolite; fdike-felsic dike; (p)and-(pillowed)andesite; (q, f)p-(quartz, feldspar) porphyritic; § 1: McGill (XRF); Ontario Geological Survey (OGS; ICPMS; 2001), 2: OGS (2001), 3: Acme (2001), 4: GSC (2003), 5: OGS (2002), 6: McGill; OGS (2003); see Rogers (2004); # b.d.-below detection; n.a. not applicable: †† Mg# = $Mg^{2+}/(Mg^{2+} + Fe^{2+})$, $Fe^{3+}/Fe^{2+} = 0.1$; ‡‡ N-MORB normalized value (Sun and MacDonough, 1989).

abundances of trace elements (fig. 6). Similar to PP_1, the samples exhibit consistently strong Th enrichment (La_n/Th_n 0.2), strong Nb depletion (La_n/Nb_n 5.7) and negative Zr and Hf anomalies (Zr_n/Sm_n 0.5). However, this geochemical type appears to lack Ti depletion, has stronger enrichment of LREE (La_n/Sm_n 3.9) and has flat HREE (Gd_n/Lu_n 1.1). PP_2 samples are primitive to moderately evolved (Mg# 70.5 to 58.7).

Table 3

Sm/Nd isotope data

Sample†	Stratigraphic unit	Type	Age	Nd‡	Sm‡	$^{143}Nd/^{144}Nd$		$^{147}Sm/^{144}Nd$	$^{143}Nd/^{144}Nd_i$§	εNd(t)§
VL01A325	Dragon Pond Fm.	WB_3	454	19.32	3.94	0.512217	(16)	0.1234	0.511850	-3.98
VL01A315#	Dragon Pond Fm.	WB_3	454	17.72	3.45	0.512194	(13)	0.1178	0.511844	-4.08
VL02A140b	Dragon Pond Fm.	WB_1	454	7.21	1.87	0.512824	(14)	0.1570	0.512357	5.93
VL02A246b	Pats Pond Group	PP_6	487	11.22	2.87	0.512701	(15)	0.1546	0.512208	3.85
VL02A221	Pats Pond Group	PP_4	487	3.12	0.85	0.512777	(14)	0.1655	0.512249	4.67
VL02A128	Pats Pond Group	PP_4	487	2.17	0.63	0.512854	(6)	0.1766	0.512291	5.48
VL02A202	Pats Pond Group	PP_1	487	10.14	2.68	0.512493	(12)	0.1598	0.511983	-0.54
VL02A026	Pats Pond Group	PP_1	487	13.04	3.30	0.512515	(15)	0.1530	0.512026	0.31

† Lithology, location and geochemistry listed in table 2; ‡ Concentration in ppm from isotope dilution; § Calculated at age of formation; # felsic tuff, no geochemical analysis, NAD83, UTM Zone 21 468729 5360774

PP_3 and PP_4 (n = 12) comprise calc-alkaline arc andesite to rhyolite (SiO_2 49 to 73 wt%; figs. 6 and 7A). The types were separated on the basis of field characteristics, however PP_3 and PP_4 have similar geochemical traits. PP_3 comprises feldspar (± quartz) porphyritic volcanic rocks, whereas PP_4 comprises quartz (± feldspar) porphyritic volcanic rocks. PP_3 and PP_4 have very similar trace and major element characteristics. Samples exhibit consistently strong Th enrichment (La_n/Th_n 0.2), strong Nb depletion (La_n/Nb_n 4.4) and generally prominent Ti depletion. Zr and Hf anomalies range from un-depleted to moderately depleted (Zr_n/Sm_n 0.8). There is strong enrichment of LREE (La_n/Sm_n 2.4) and moderate depletion of MREE (Gd_n/Lu_n 0.75) resulting in a characteristic concave-up profile for these samples on N-MORB normalized spidergrams (fig. 7). The two types may be differentiated geochemically on the basis of the slope of HREE (Gd_n/Lu_n 2.6 (PP_3); 2.1 (PP_4)). PP_3 and PP_4 samples are moderately to strongly evolved (Mg# 47 to 56 (PP_3), 42 to 51 (PP_4)). Sm-Nd isotopic analysis of two PP_4 samples yielded εNd_{487} values of +4.7 and +5.5 (table 3). The felsic rocks of this suite plot in the volcanic arc field on a Yb – Ta plot (fig. 7A; Pearce and others, 1984).

PP_5 is represented by a single moderately evolved (Mg# 57) sample of IAT that exhibits strong Th enrichment and prominent Nb depletion. There is slight enrichment of LREE (La_n/Sm_n 1.4) and slight depletion of MREE (Gd_n/Lu_n .85). This sample plots on the intersection of MORB – BAB – VAB fields La/10-Y/15-Nb plot (fig. 7A; Cabanis and Lecolle, 1989).

PP_6 (n = 2) comprises high silica trondhjemitic (O'Connor, 1965) rhyolite (SiO_2 80 to 83 wt%). Samples exhibit strong Th enrichment ($La/_nTh_n$ 0.1), prominent Nb depletion (La_n/Nb_n 2.3), and strong Eu and Ti depletion. There are prominent positive Zr and Hf anomalies (Zr_n/Sm_n 1.4), strong enrichment of LREE (La_n/Sm_n 3.2) and prominent depletion of MREE (Gd_n/Lu_n 0.66). The samples are strongly evolved (Mg# 34 to 43). Sm-Nd isotopic analysis of one sample yielded an εNd_{487} value of +3.89 (table 3). The rocks of this suite plot on the boundary of arc and ocean ridge granite fields on the Yb – Ta plot (fig. 7A; Pearce and others, 1984).

Wigwam Brook Group

The Dragon Pond Formation of the Wigwam Brook Group comprises five distinct informal geochemical types of volcanic rocks, referred to herein as WB_1 to WB_5. WB_1 is a high silica rhyolite (n = 2; SiO_2 76 to 84 wt%) and occurs near the base of the Dragon Pond Formation (figs. 6 and 7B). The samples exhibit strong Th (La_n/Th_n 0.2), Nb (La_n/Nb_n 0.5) and LREE (La_n/Sm_n 2.9) enrichment. Ti is strongly depleted, as is Eu in one sample. Sm-Nd isotopic analysis of one sample yielded an εNd_{454} value of +6.0 (table 3). The samples plot in the within-plate field on granitoid discrimination plots (fig. 7; Pearce and others, 1984).

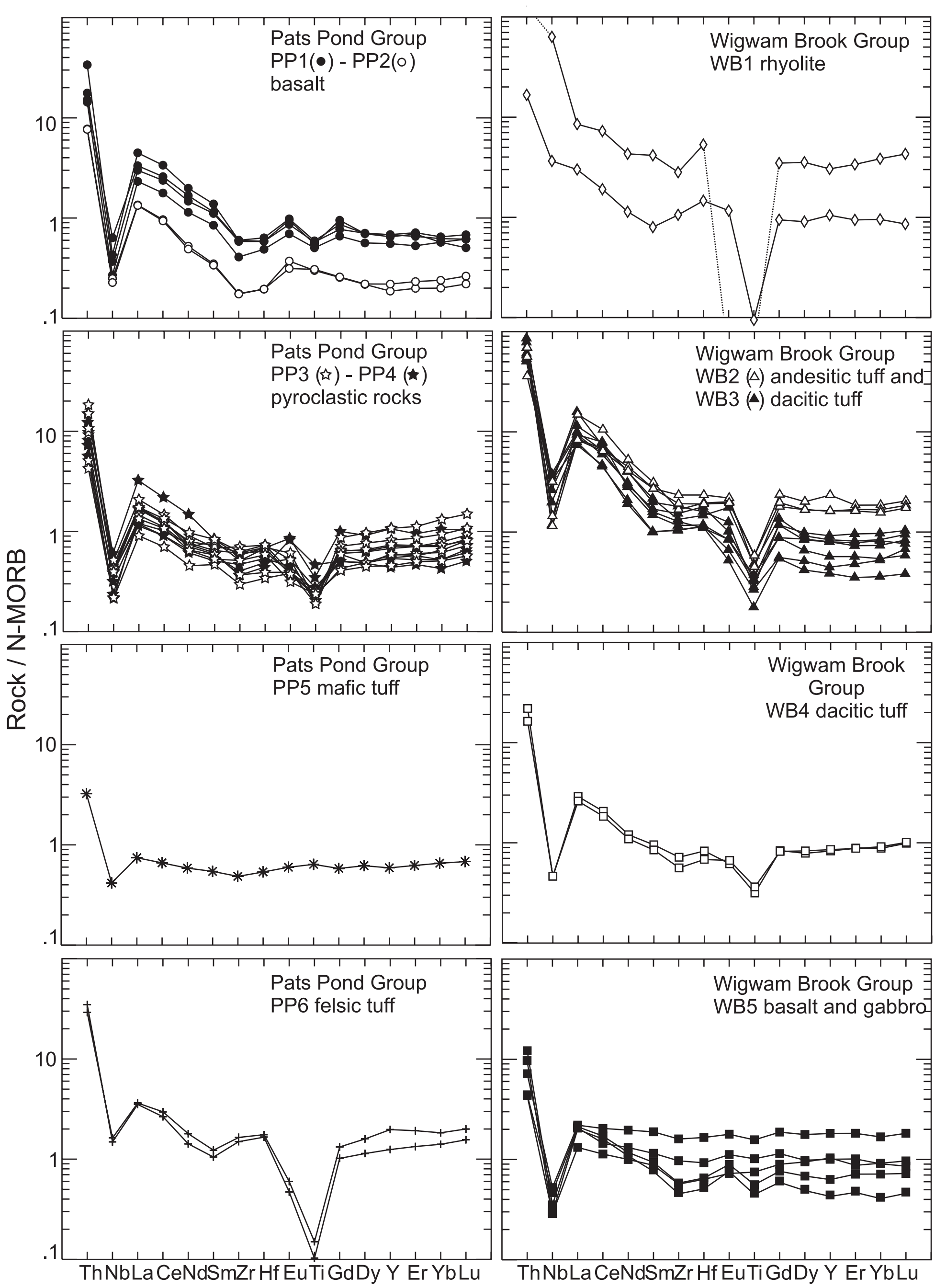

Fig. 6. Extended trace-element normalized plots for the Pats Pond and Wigwam Brook groups (N-MORB normalized, Sun and McDonough, 1989).

WB_2 is andesitic (n=3; SiO_2 60 to 64 wt%) and occurs throughout the Dragon Pond Formation interlayered with group WB_3 rhyodacite (figs. 6 and 7B). The samples exhibit consistently strong Th enrichment (La_n/Th_n 0.2), strong Nb (La_n/Nb_n 5.9)

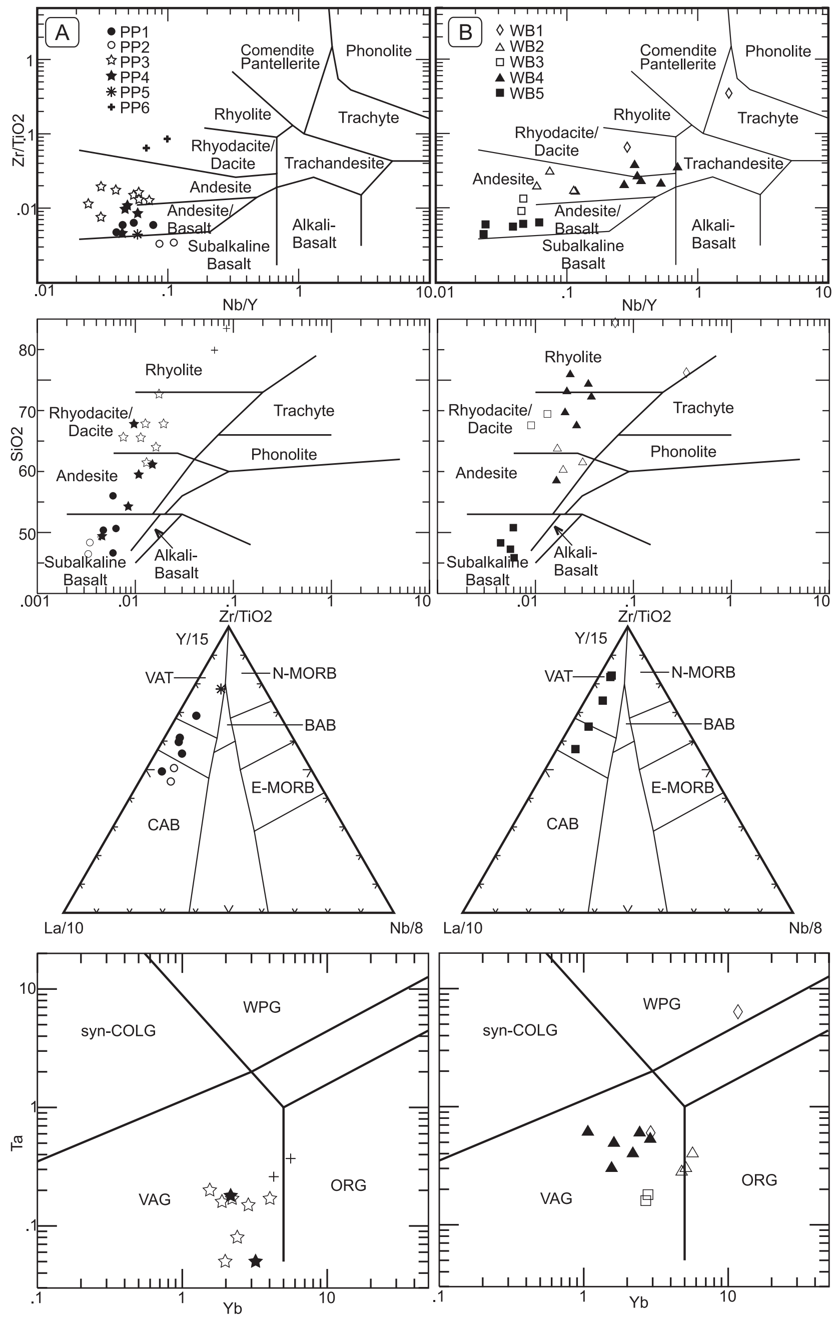

Fig. 7. Nb/Y vs. Zr/TiO_2 rock type classification (Winchester and Floyd, 1977), La/10-Y/15-Nb/8 (Cabanis and Lecolle, 1989) and Yb vs. Ta (Pearce and others, 1984) tectonic discrimination diagrams for Pats Pond and Wigwam Brook groups. BAB – backarc basin basalt, CAB – calc-alkaline basalt, E-MORB – enriched mid-oceanic ridge basalt, N-MORB – normal mid-oceanic ridge basalt, ORG – ocean ridge granite, syn-COLG – syn-collision granite, VAG – volcanic arc granite, VAT – volcanic arc tholeiite, WPG – within-plate granite.

and Ti depletion, prominent negative Zr and Hf anomalies (Zr_n/Sm_n 0.70) and strong enrichment of LREE (La_n/Sm_n 3.7) and flat HREE profile (Gd_n/Lu_n 1.1). The andesite is moderately evolved (Mg# 46 to 51). WB_2 samples plot on the boundary of the volcanic arc and ocean ridge/within plate granite field on granitoid discrimination plots (fig. 7B; Pearce and others, 1984).

WB_3 andesite to rhyodacite (n = 7; SiO_2 58 to 74 wt%) exhibit consistently strong Th enrichment (La_n/Th_n 0.2), strong Nb depletion (La_n/Nb_n 4.3), strong Ti depletion, slight negative Zr and Hf anomalies (Zr_n/Sm_n 0.9) and strong enrichment of LREE (La_n/Sm_n 6.7) and slight enrichment of MREE (Gd_n/Lu_n 1.3). This geochemical type is strongly fractionated (Mg# 16 to 50). The sample analyzed for its Sm-Nd isotope composition was collected immediately above the breccia horizon and yielded an εNd_{454} of −4.0 (table 3). A second sample, which was collected stratigraphically below the breccia horizon, yielded an εNd_{454} of −4.1. Although the geochemistry of this sample was not determined, the measured Sm-Nd ratio of <0.2 is consistent with other samples in this group (>0.2 in WB_2). WB_3 samples plot in the volcanic arc granite field on granitoid discrimination plots (fig. 7B; Pearce and others, 1984).

WB_4 type comprises dacitic tuff (n = 2; SiO_2 67 to 69 wt%). The samples occupy an uncertain stratigraphic position in the northeastern part of the Wigwam Brook Group and are associated with rocks typical of the Dragon Pond Formation (figs. 6 and 7B). WB_4 is characterized by strong Th enrichment (La_n/Th_n 0.2), strong Nb (La_n/Nb_n 6.0) and Ti depletion, slight negative Zr and Hf anomalies (average Zr_n/Sm_n 0.7) and strong enrichment of LREE (La_n/Sm_n 3.1) and slight enrichment of HREE (Gd_n/Lu_n 0.8). WB_4 samples are strongly evolved (Mg# 33 to 42). They plot in the volcanic arc granite field on granitoid discrimination plots (fig. 7B; Pearce and others, 1984).

WB_5 comprises several analyses of tholeiitic basalt (n = 4) and gabbro (n = 1; figs. 6 and 7B). The samples exhibit Th enrichment (La_n/Th_n 0.2 to 0.5), strong Nb depletion (La_n/Nb_n 4.2 to 6.9), negative Zr and Hf anomalies (Zr_n/Sm_n 0.6 to 0.8), prominent enrichment of LREE (La_n/Sm_n 1.2 to 2.6), slight enrichment to slight depletion of HREE (Gd_n/Lu_n 0.9 to 1.3). The samples plot in the field transitional between calc-alkaline basalt and island arc tholeiite on the La-Y-Nb discrimination plot (fig. 7B; Cabanis and Lecolle, 1989).

DISCUSSION

The Pats Pond and Wigwam Brook groups form the western most portion of the peri-Gondwanan Victoria Lake Supergroup (fig. 1). The adjacent rocks of the Red Indian Lake Group to the west display peri-Laurentian affinities (Zagorevski and others, 2006) including lack of Upper Ordovician black shale cover and a sub-Silurian unconformity (see Williams and others, 1988). Hence the Wigwam Brook and Red Indian Lake groups (fig. 1) are separated by the Red Indian Line, which is conveniently marked by black shale melange (Rogers and van Staal, 2002). In the following section, the tectonic setting and correlatives of the Pats Pond and Wigwam Brooks groups will be discussed and they will be placed into a regional tectonic framework. This enables an alternative tectonic model (van Staal, 1994) to be proposed for the Victoria Lake supergroup and related tectonic elements in Newfoundland. This model is applicable to the temporally correlative belts in New Brunswick, Nova Scotia and Maine.

Pats Pond Group and Correlatives

The c. 487 Ma age of the Pats Pond Group is distinctly younger than the adjacent rocks of the Cambrian Victoria Lake supergroup (fig. 1; c. 513 – 494 Ma; Evans and others, 1990; Dunning and others, 1991; Evans and Kean, 2002) from which it is separated by a high strain zone interpreted to be a steepened thrust. The Pats Pond Group preserves a chemical stratigraphy that is entirely consistent with a supra-subduction zone origin. The transitional tholeiitic to calc-alkaline basalt (PP_1, PP_2) in the lower and middle Pats Pond Group has a strong arc signature, as indicated by Th and LREE enrichment and Nb depletion. Intermediate and felsic rocks higher in the stratigraphy (PP_3, PP_4) display similar characteristics indicative of an arc volcanic setting. On the other hand, the stratigraphically highest IAT (PP_5) and trondhjemitic rhyolite (PP_6) have a relatively weak arc signature, suggesting a transitional setting between an arc and back-arc environment (figs. 6 and 7A). The upward transition from arc to back-arc in the Pats Pond Group is interpreted to represent the progressive rifting of a dominantly extensional calc-alkaline arc.

Temporal equivalents to the Pats Pond Group occur in north-central Newfoundland and include the Exploits Group (c. 486 Ma, O'Brien and others, 1997), Wild Bight Group and South Lake Igneous complex (c. 489 – 486 Ma, O'Brien, 1992; MacLachlan and Dunning, 1998a), and New Bay Pond sequence (Swinden and Jenner, 1992). These record transitions from arc tholeiite to trondhjemitic rhyolite to refractory back-arc tholeiite (O'Brien and others, 1997), refractory arc tholeiite to boninite to non-arc tholeiite (MacLachlan and Dunning, 1998a), and refractory arc tholeiite to non-arc tholeiite (Swinden and Jenner, 1992), respectively.

The eruption of boninite ($\pm$ refractory arc tholeiite) can be favored by many tectonic settings characterized by high heat flow, including initiation of subduction (for example, Stern and Bloomer, 1992), forearc spreading (for example, Bedard and others, 1998), mantle plume (for example, Sobolev and Danyushevsky, 1994; Macpherson and Hall, 2001), and intersection of a subduction zone and spreading ridge (for example, Falloon and Crawford, 1991; Monzier and others, 1993). Presence of older arc volcanism in the Victoria Lake supergroup (Evans and Kean, 2002) discounts the subduction initiation model of MacLachlan and others (1998a). Forearc spreading is a very rare tectonic setting with no modern analogues (Fryer and Pearce, 1992) and is probably associated with initiation of subduction. In recent arcs, boninite and refractory tholeiite eruption is commonly associated with the propagation of a back-arc spreading center into an active arc (for example, Tonga: Falloon and Crawford, 1991; New Hebrides: Monzier and others, 1993). Coeval eruption of calc-alkaline basalt (Pats Pond group: see previous) and boninite and refractory tholeiite (Wild Bight Group: MacLachlan and Dunning, 1998a), as well as presence of sheeted diabase (O'Brien, 1992; MacLachlan and Dunning, 1998a) strongly suggests active rifting of an arc, probably as a result of intersection of a backarc-spreading center with the active arc. This arc is referred to as the Penobscot Arc in northern Appalachians (van Staal and others, 1998).

Penobscot Arc Characteristics

The Penobscot arc was generally accepted to be an ensimatic arc system in the Newfoundland Appalachians (for example, Swinden and Jenner, 1992; O'Brien and others, 1997; MacLachlan and Dunning, 1998a). However, geochronology of the Pats Pond Group has revealed significant Proterozoic zircon inheritance. Presence of xenocrystic zircon, in the c. 560 Ma and c. 0.9 to 1.2 Ga age range, is consistent with the presence of Gander-like crust in the source (for example, van Staal and others, 1996; McNicoll and others, 2001, 2003; Rogers and others, 2006).

The age of the youngest xenocrystic zircon is identical to the nearby, continentally contaminated Crippleback Igneous Suite and related Sandy Brook Group (figs. 8 and 9; Evans and others, 1990; Kerr and others, 1995; Rogers and others, 2006) suggesting that Pats Pond Group was built on related crust. Although no zircon inheritance has been identified in the Crippleback Igneous Suite, the Sm-Nd isotopic data indicate c. 1.1 to 1.3 Ga T_{DM} ages (Kerr and others, 1995) consistent with presence of Mesoproterozoic crust in the source region similar to the older population of xenocrystic zircon in the Pats Pond Group. We thus interpret the Pats Pond group to have erupted in an

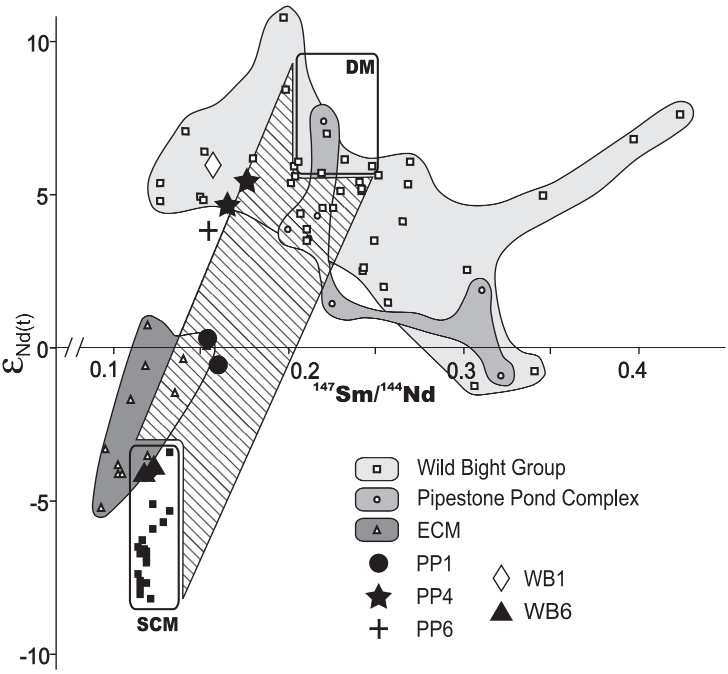

Fig. 8. ε_{Nd} versus $^{147}Sm/^{144}Nd$ plot illustrating the range of values in the Lower Ordovician Pats Pond and Upper Ordovician Wigwam Brook groups. The range of values in Lower Ordovician Wild Bight Group (Swinden and others, 1990; MacLachlan and Dunning, 1998a), Upper Cambrian Pipestone Pond Complex (Jenner and Swinden, 1993) is plotted for reference. Field with diagonal lines illustrates mixing trend between SCM and DM. ECM (exposed continental material), SCM (subducted continental material), DM (depleted mantle); see text for discussion.

ensialic arc setting above attenuated Crippleback basement. Crippleback Igneous Suite has been recently proposed to form a remnant of Ganderian basement in central Newfoundland (Rogers and others, 2006).

Low εNd values (-0.5 to +0.3) in the Pats Pond mafic lavas (PP_1) likewise support interaction with mature continental crust. The role of continental material in the genesis of the Pats Pond Group can be qualitatively investigated using the Sm-Nd isochron diagram to illustrate possible mixing/partial melting relationships (fig. 8). Three hypothetical sources are used in the discussion of the isotopic data: depleted mantle (DM), subducted continental material (SCM), and exposed continental material (ECM). The DM field for the Tremadocianian mantle, based on the composition of Ordovician ophiolitic rocks in Newfoundland, is from Jenner and Swinden (1993). The SCM field represents the range of Gander Zone meta-sedimentary rocks that could have been subducted in the Tremadocian and is also representative of the Gander Zone continental basement (compiled from D'Lemos and Holdsworth, 1995; Kerr and others, 1995; Whalen and others, 1997; compare Jenner and Swinden, 1993). The ECM field is derived from the exposed Proterozoic igneous and volcanic rocks (fig. 9; Crippleback Intrusive Suite and Sandy Brook Group: Kerr and others, 1995; Rogers and others, 2006) that may represent portions of the basement to the Penobscot Arc (Rogers and others, 2006). The ECM has a lower $^{147}Sm/^{144}Nd$ ratio and higher εNd values than the SCM.

The PP_1 calc-alkaline basalt plots within a mixing field between DM and SCM/ECM sources. A simple mixing relationship is consistent with the high Mg# (66.5 and

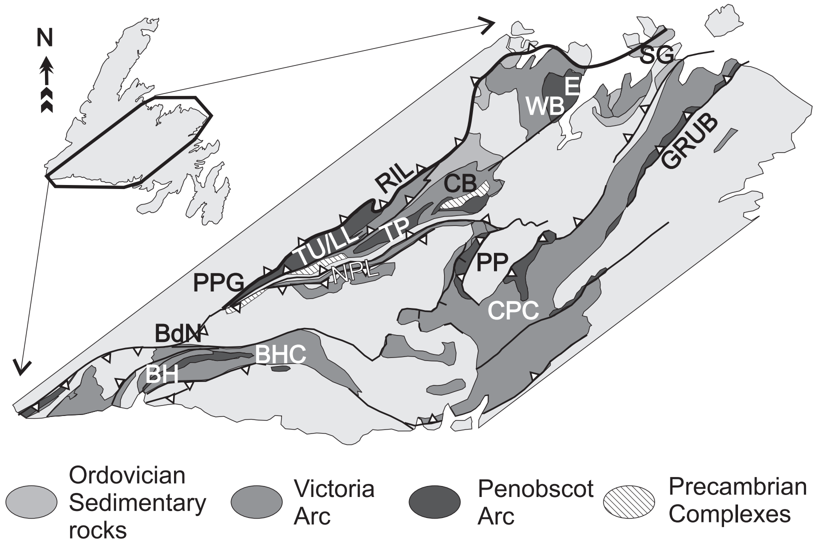

Fig. 9. Distribution of pre-Cambrian Suites, Cambro-Ordovician Penobscot arc, and Ordovician Victoria arc complexes in Newfoundland (after van Staal and others, 1998). BdN – Bay du Nord Group; BH – Baggs Hill Granite; CB – Crippleback Igneous Suite and Sandy Lake Group; E – Exploits Group; LL – Long Lake group; NPL – Noel Paul's Line; PPG – Pats Pond Group; RIL – Red Indian Line; SG – Summerford Group; TP- Tally Pond Group; TU – Tulks; WB - Wild Bight Group. Penobscot ophiolites: BHC – Blue Hills of Couteau ophiolite Complex; CPC – Coy Pond Complex; GRUB – Gander River Ultrabasic Belt; PP – Pipestone Pond Complex.

70.5) indicating that the basalts likely represent relatively unfractionated liquids. PP_4 felsic rocks have lower $^{147}Sm/^{144}Nd$ than would be expected if a simple mixing model of the DM and SCM source components were assumed. An addition of a third component, such as a low-degree partial melt of either DM or SCM (similar to ECM), could easily explain the observed data.

Similar to Pats Pond Group, Sm-Nd isotope data of the Wild Bight Group (Swinden and others, 1990a; MacLachlan and Dunning, 1998a) indicate influence of continental material in the source area of the magmatic rocks of the Penobscot Arc although a highly depleted source characterized by high $^{147}Sm/^{144}Nd$ is required. In the absence of clear zircon inheritance in the Wild Bight Group, the low ε_{Nd} values have been interpreted to represent contamination of the magma source region by subduction of continentally–derived sedimentary material (MacLachlan and Dunning, 1998a). An entirely ensimatic setting for the Wild Bight and Exploits groups would require a transition from continental (that is Pats Pond group) to oceanic arc substrate along strike of the Penobscot Arc, and trench parallel transport of arc and basement-derived sediment from areas of ensialic magmatism (*see following*). Such a transition would generally reflect major irregularities in the Gander continental margin relative to the strike of the arc (for example, Kermadec Arc: Gamble and others, 1995) and can be explained by local transgression of the Penobscot Arc onto oceanic crust adjacent to such irregularities in the margin during arc-trench migration. Alternatively, the Wild Bight Group could represent advanced stages of rifting of an ensialic magmatic arc formed as a result of intersection of a backarc spreading center with the active arc (for example, Tonga: Falloon and Crawford, 1991; New Hebrides: Monzier and others, 1993).

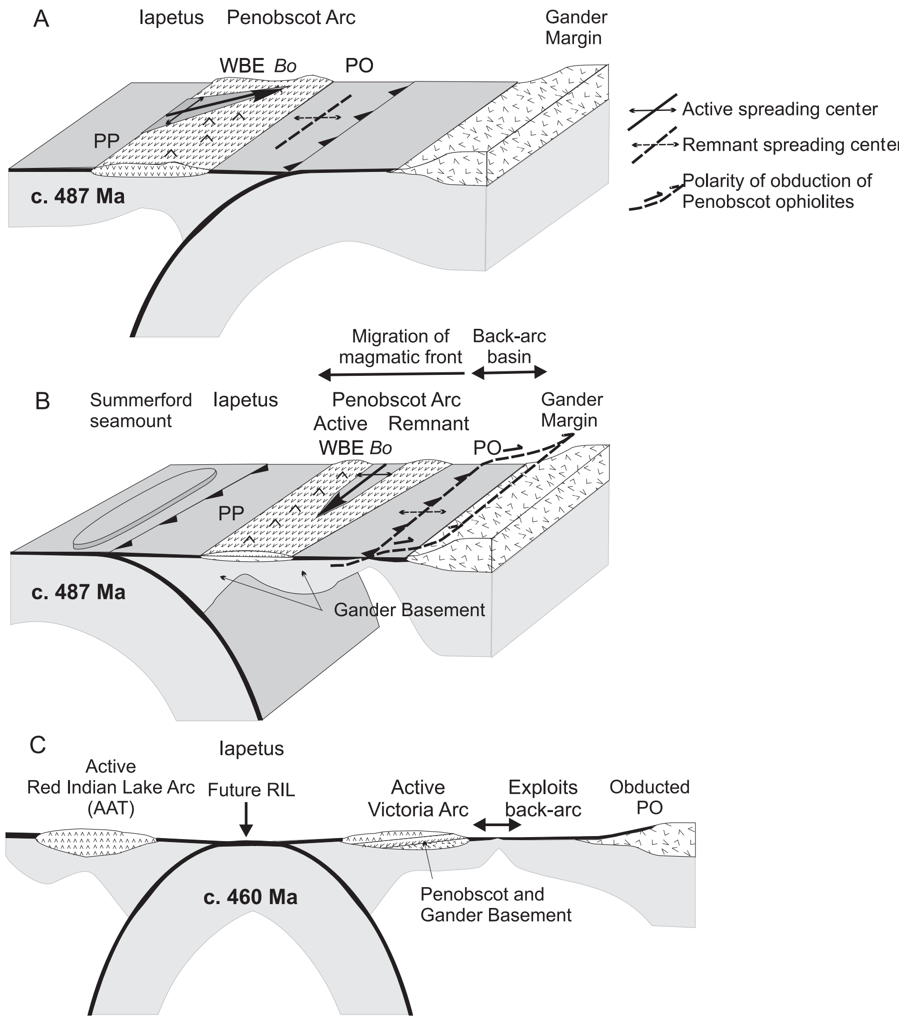

Fig. 10. Upper Cambrian tectonic evolution of the Penobscot arc (A-B) and its convergence with the Gander margin; and Upper Ordovician tectonic evolution of the Victoria Lake arc (C) and its convergence with the peri-Laurentian Red Indian Lake arc and Annieopsquotch Accretionary Tract (AAT). (A: modified from van Staal, 1994) and (B) represent alternate models for obduction of Penobscot ophiolites onto the Gander margin. Bo – boninite; PO – Penobscot Ophiolites; PP – Pats Pond Group; WBE – Wild Bight and Exploits Group.

Evolution of the Penobscot Arc

The Cambrian to Lower Ordovician portions of the Victoria Lake supergroup, which includes the Pats Pond Group, form part of the extensive Penobscot Arc system that extends from Newfoundland to Maine (van Staal and others, 1998). Previous models of the Penobscot arc (fig. 10) have attempted to reconcile the obduction of the Penobscot ophiolites with a west-dipping subduction of the Gander margin (van Staal, 1994), and the Penobscot arc was generally assumed to be ensimatic (for example Swinden and Jenner, 1992; O'Brien and others, 1997; MacLachlan and Dunning, 1998a). Improved understanding of the provenance and significance of the Victoria Lake supergroup and the adjacent units in Newfoundland allows us to evaluate the tectonic models for the Penobscot Arc system.

In the Victoria Lake supergroup, the arc complexes become progressively younger towards the Red Indian Line (fig. 1). From east to west these include Tally Pond (c. 513 Ma: Dunning and others, 1991; Rogers and others, 2006), Long Lake (c. 505 Ma: McNicoll, unpublished data; van Staal and others, 2005c), Tulks (c. 498 Ma: Evans and others, 1990) and Pats Pond groups (c. 487 Ma; *see above*). Similarly, the Wild Bight and Exploits groups (c. 486 – 489 Ma) are also located along the Red Indian Line in north-central Newfoundland. Although such a distribution could be due to a complicated deformation history, the lack of repetition of tectonic units and only sparse magmatic links suggest that this more likely reflects the original relative positioning of these magmatic phases, such that they formed during the trench-ward migration of the magmatic front. The temporal and spatial changes in the magmatic front can be utilized to reconstruct the geometry and evolution of the subduction zones in ancient orogens (for example Şengor and Natal'in, 1996). Hence, since the Tremadocian volcanic sequences of the Penobscot arc should be situated trench-ward from the Cambrian volcanic sequences, the trench should lie to the west (figs. 9 and 10B). Consistent with the proposed trench location, the Penobscot ophiolites (figs. 9 and 10B; c. 494 Ma: Dunning and Krogh, 1985), which have been interpreted to have formed in a back-arc tectonic setting (Jenner and Swinden, 1993) are currently positioned to the east of the Cambro-Ordovician Penobscot Arc (fig. 10B).

If the interpretation of the relationships between the arc-back-arc complexes is valid, then their present distribution suggests that the Penobscot Arc was formed above an east dipping (present coordinates) subduction zone (fig. 10B). The earliest known supra-subduction zone magmatism is c. 513 Ma (Tally Pond Group in Newfoundland; Dunning and others, 1991; Rogers and others, 2006; Mosquito Lake Formation in New Brunswick: Johnson and McLeod, 1996; McLeod and others, 2003), and was located along an attenuated or perhaps irregular Gander margin (fig. 10B). The presence of Gander margin is indicated by basement-cover relationships (van Staal, 1994; Johnson and McLeod, 1996; Rogers and others, 2006), zircon inheritance data (Squires and Moore, 2004) and Sm-Nd isotopic characteristics (figs. 8 and 11; Rogers and others, 2006). Ensialic arc volcanism (for example, Rogers, 2004) was occurring until c. 494 Ma, when the Penobscot back-arc basin was formed (Jenner and Swinden, 1993) separating the ensialic Penobscot arc from its parent (Ganderian) microcontinent. Similar to the ensialic portions of the Penobscot Arc, the Penobscot back-arc basin ophiolites show evidence of contamination by crustal material (Pipestone Pond Complex: fig. 8; ε_{Nd} 7.3 to -1.3: Jenner and Swinden, 1993) suggesting rifting of an ensialic basement. Following the rifting event, calc-alkaline ensialic arc volcanism was re-established by c. 490 Ma (Pats Pond Group) while portions of the Penobscot arc were still undergoing active extension (fig. 10B; for example, Wild Bight Group: Swinden and others, 1990; MacLachlan and Dunning, 1998a; Exploits Group: O'Brien and others, 1997).

A prominent magmatic gap in the arc-magmatism in the Exploits Subzone (c. 485 – 480 Ma; van Staal and others, 1998) coincides with the obduction of the Penobscot back-arc basin ophiolites onto the Gander passive margin prior to c. 478 Ma (fig. 10B; Colman-Sadd and others, 1992; Tucker and others, 1994) and an unconformity on the Gander Zone in Newfoundland and east-central Maine (Boone and others, 1989). Previously this has been interpreted to mark the arc-continent collision with the west-dipping subduction attached to the Gander Margin (fig. 10A; van Staal and others, 1996; MacLachlan and Dunning, 1998a) . However this is inconsistent with the east-dipping subduction zone model proposed herein where Gander margin is never subducted (fig. 10B).

The cause of the inversion of the Penobscot back-arc basin is incompletely understood at present, however the obduction of the ophiolites occurred while the

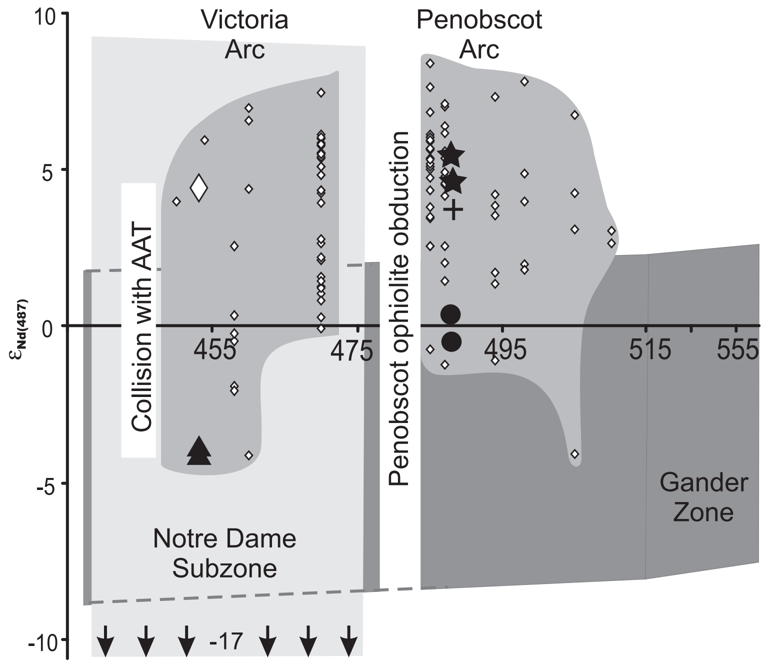

Fig. 11. Diagramatic illustration of the Nd isotopic evolution of the arc – back-arc complexes of the Penobscot and Victoria Lake arcs based on ε_{Nd} plotted versus age. Field for Notre Dame Subzone (light gray) plotted for reference (data from Swinden and others, 1990, 1997; Jenner and Swinden, 1993; Kerr and others, 1995; Whalen and others, 1997, 1998; MacLachlan and Dunning, 1998a, 1998b; Rogers, 2004; Rogers and others, 2006).

backarc was still young (<10 My). Investigations of the structure of young ensialic back-arc basins indicate that they develop a strong asymmetry with the spreading concentrated near the magmatic front, where the lithosphere is the weakest (for example, Barker and others, 2003). This inherent asymmetry favors the obduction of back-arc crust onto the continental margin if the ensialic arc and young back-arc are placed under compression (for example, Rocas Verdes: Dalziel, 1986; Barker and others, 2003). Compression of the arc can be caused by a change in plate motions (Andean orogenesis: Dalziel, 1986) and/or collision with thickened crust, such as an oceanic plateau (for example, Cloos, 1993). The incomplete understanding of the Ordovician plate motions precludes any inferences to be made about the former, although evidence for a Tremadocian outboard collision event may be preserved in the Notre Dame Bay area of Newfoundland. The Summerford Group basalts (fig. 9; at least Tremadocian: Kay, 1967) have been interpreted as remnants of a seamount(s) (Jacobi and Wasowski, 1985) which was accreted to the Penobscot along the Red Indian Line and incorporated into the Dunnage melange (van Staal and others, 1998). The original aerial extent of the seamount or plateau represented by the Summerford Group is unknown as only the upper portion of the crust is likely to be incorporated into the accretionary complex (for example, Kimura and Ludden, 1995) while the rest would be generally subducted (for example, Cloos, 1993). Hence, the capability of the Summerford Group to place the Penobscot arc under compression leading to inversion of the back-arc is only a speculation, although it can certainly be a viable cause for the Penobscot Orogeny and accompanying magmatic gap. Alternate models may involve subduction of young oceanic lithosphere and/or spreading center. Following the inversion of the back-arc basin and obduction of the Penobscot ophiolites, felsic arc-related plutons intruded the Gander margin and stitched the ophiolites by 478 to 474 Ma (for example, Colman-Sadd and others, 1992; Tucker and others, 1994), placing an upper age constraint on the age of the Penobscot Orogeny in Newfoundland.

Tectonic Setting of the Wigwam Brook Group

The Wigwam Brook Group is the youngest known tectono-stratigraphic unit in the Victoria Lake supergroup. The Wigwam Brook Group probably unconformably overlies the Pats Pond Group, indicating deposition above Penobscot Arc basement. Chemistry of the volcanic rocks indicates that there are two distinct tectonic settings preserved in the basal Dragon Pond Formation. High silica rhyolite (WB_1) near the base of the Dragon Pond Formation lacks an arc signature and plots in part in the within-plate field on a granitoid tectonic discrimination diagram (fig. 7; Pearce and others, 1984), and could have erupted in a tectonic setting such as rifting of an ensialic arc. The age of eruption of WB_1 rhyolite is poorly constrained at present, it may be significantly older than the overlying volcanic rocks (Williams and others, 1993). The proposed extensional setting is consistent with the dominantly extensional evolution of the Victoria Arc in the Middle Ordovician (for example, O'Brien and others, 1997; MacLachlan and Dunning, 1998b; van Staal and others, 1998). Alternatively, this unusual chemistry may be related to ridge subduction as inferred for the broadly correlative portions of the Bathurst supergroup of New Brunswick (Rogers and van Staal, 2003; Rogers and others, 2003; van Staal and others, 2003).

Felsic volcanic rocks that are geochemically different were deposited above the WB_1 rhyolite and associated volcanoclastic sediments. $WB_{2\text{-}4}$ andesitic and dacitic rocks exhibit LREE enrichment and Nb depletion consistent with derivation in a volcanic arc setting, although this could also be an inherited characteristic of volcanic arc-related basement. The low εNd values (-4.0) in WB_3 dacite indicate strong influence of mature continental crust (T_{DM} ~1370 Ma), either in the source and/or as a result of contamination by continentally-derived sediment during deposition. The associated mafic volcanic rocks near the top of the Dragon Pond Formation also suggest eruption in a volcanic arc setting. The predominantly felsic volcanic activity, combined with very low εNd values, zircon inheritance and basement-cover relationships, indicate eruption of the Dragon Pond Formation in a mature ensialic arc setting above composite Penobscot and Gander basement.

The upper portions of the Dragon Pond Formation record waning volcanic activity, suggesting a significant change in tectonic environment. The overlying Halfway Pond and Perrier's Pond Formations are predominantly sedimentary. Shale and immature wacke comprise the Halfway Pond Formation, while shale and black shale dominate the Perrier's Pond Formation. The transition from Dragon Pond Formation to Halfway Pond and Perrier's Pond formations is interpreted to represent the cessation of ensialic arc volcanism. Cessation of arc volcanism is well documented in the Exploits Subzone and the predominantly volcanic Victoria Lake supergroup is overlain by marine black shale and turbidite sequence of the Upper Ordovician to Llandovery Badger Group (Williams and others, 1993).

Evolution of the Victoria Arc

Following the Penobscot Orogeny, Middle to Upper Ordovician rocks of the Victoria Lake supergroup were deposited on the composite Penobscot - Gander basement. Volcanic rocks of the Victoria Lake supergroup were erupted in various arc-related settings related to the Victoria Arc magmatism in central Newfoundland (for example, Evans and Kean, 2002). The oldest dated felsic ensialic arc volcanic rocks in the Victoria Lake supergroup are contained in a structural panel immediately to the east of the Wigwam Brook Group (c. 453 Ma), within the c. 462 Ma (Dunning and others, 1987) Sutherlands Pond Group (fig. 1; Rogers and others, 2005b), which contains E-MORB-like basalt (Upper Basalts: Evans and Kean, 2002). Coeval calc-alkaline arc felsic and E-MORB mafic magmatism suggests the presence of an immature back-arc basin to the east of the Wigwam Brook arc volcanics. Further to the east, the Middle Ordovician Diversion Lake Group (not shown; Kean and Mercer, 1981) basalts and Harpoon Gabbro intrusive suite (fig. 1; 465±2: Pollock and others, 2002, 2004) have enriched within plate characteristics with tholeiitic and calc-alkaline affinities suggestive of rifting of ensialic basement (Pollock and Wilton, 2001; Evans and Kean, 2002). While the Red Cross Group (Valverde-Vaquero and others, 2006), situated along the Noel Pauls Line (fig. 9), is most likely a correlative of the Bathurst Supergroup in New Bruswick (van Staal and others, 2003), which represents the Exploits – Tetagouche backarc basin (fig. 10B). Similar to the Penobscot arc (see previous), this configuration most simply reflects the location of the trench to the west of the arc – back-arc, that is along or underneath the Red Indian Line (fig. 10C).

Correlative arc sequences to the Victoria Arc include the Wild Bight-Exploits Arc and back-arc in the north-central Newfoundland (MacLachlan and others, 2001) and Popelogan Arc – Tetagouche back-arc in New Brunswick (van Staal and others, 1998). The oldest Victoria arc-related supra-crustal rocks in Newfoundland include the Upper Wild Bight Group (fig. 9; c. 473 Ma: MacLachlan and Dunning, 1998b) and Upper Exploits Group (fig. 9; Arenig: O'Brien and others, 1997). The Wild Bight Group records the establishment of ensialic calc-alkaline arc magmatism above composite Gander and Penobscot basement and subsequent rifting of this arc (MacLachlan and Dunning, 1998b). The adjacent Exploits Group also records opening of a back-arc in which the sedimentation was active until at least Upper Ordovician (O'Brien and others, 1997). Similarly, calc-alkaline magmatism was established in the Popelogan Arc in New Brunswick by c. 474 Ma (for example, Rogers and others, 2003) followed by the opening of the Tetagouche back-arc basin (for example, van Staal and others, 1998; Rogers and van Staal, 2003).

The distribution of the Popelogan – Victoria Arc and Exploits – Tetagouche back-arc complexes indicates east-dipping subduction underneath the Gander margin, which culminated in the opening of the wide Japan Sea-like Exploits – Tetagouche back-arc basin (fig. 10; for example, van Staal, 1994; O'Brien and others, 1997; van Staal and others, 1998; MacLachlan and others, 2001; Rogers and van Staal, 2003). Volcanism and sedimentation in the Victoria – Popelogan Arc and Exploits – Tetagouche back-arc were active until the Upper Ordovician, followed by a general cessation of arc volcanism (Victoria Arc: see above, Williams and others, 1993; Popelogan Arc: van Staal and others, 1991), syn-tectonic sedimentation (Badger Group: Williams and others, 1993), and the unroofing of the peri-Gondwanan (van Staal and others, 1991) and peri-Laurentian (for example, Kean, 1983; Dunning and others, 1987; Bostock, 1988) arc complexes. Subsequently deposited syn-tectonic sedimentary rocks in the Exploits Subzone contain a detrital contribution from both the Notre Dame Arc and Laurentian basement (Badger Group: Nelson, 1981; McNicoll and others, 2001). This evidence suggests Upper Caradoc collision of the peri-Gondwanan Victoria – Popelogan arc and the peri-Laurentian Annieopsquotch Accretionary Tract along the Red Indian Line and closure of the main tract of Iapetus (van Staal and others, 1998; Zagorevski and others, 2006).

CONCLUSIONS

Two new peri-Gondwanan tectono-stratigraphic units, the Tremadocian Pats Pond Group and probably unconformably overlying Caradoc Wigwam Brook Group, have been identified through detailed mapping, geochemistry and geochronology in the Victoria Lake supergroup in Newfoundland. The Pats Pond and Wigwam Brook groups define the western-most extent of the Victoria Lake supergroup and the position of the Red Indian Line. They also preserve the last stages of volcanism and sedimentation of the Penobscot and Victoria arcs and provide constraints on the evolution of these two arc systems. The tectonic model for the Penobscot Arc presented herein differs from the previously proposed models in that the ensialic Penobscot Arc was built above an east-dipping (present coordinates) subduction zone along the Gander margin. Ensialic Penobscot arc volcanism was active from 513 to 485 Ma, and at least in part was accompanied by opening up of a back-arc basin (fig. 10B). Obduction of the back-arc ophiolites onto the Gander Margin at 485 to 480 Ma and the local formation of unconformities on the Gander margin mark the Penobscot Orogeny, which formed in response to closing the back arc basin and resulted in an arc magmatic gap. Calc-alkalic arc magmatism was re-established above an east dipping subduction zone by at least c. 473 Ma (fig. 10B; for example, MacLachlan and Dunning, 1998b; Rogers and others, 2003). The Popelogan – Victoria Arc formed in a generally extensional setting, as indicated by the eruption of coeval non-arc volcanic rocks, and the formation of the wide Japan Sea-like Exploits – Tetagouche back-arc basin (fig. 10C; van Staal, 1994; O'Brien and others, 1997; MacLachlan and Dunning, 1998b; van Staal and others, 1998; Rogers and others, 2003). Magmatism and sedimentation in the Victoria – Popelogan Arc and Tetagouche-Exploits back-arc (Dunning and others, 1987; O'Brien and others, 1997; MacLachlan and Dunning, 1998b; Rogers and van Staal, 2003; Rogers and others, 2003) continued until the Caradoc collision with the Peri-Laurentian Red Indian Lake Arc (van Staal and others, 1998; Zagorevski and others, 2006), marking the closure of the main portion of Iapetus and the arrival of the leading edge of Ganderia to the Laurentian margin. Subsequently, subduction stepped back into the Tetagouche – Exploits back-arc basin, closing the remainder of the Iapetus by the end of Early Silurian (fig. 10C; for example, van Staal and others, 1998), which led to the Salinic Orogeny.

Acknowledgments

We are honored to form part of this special issue dedicated to the life achievement of John Rodgers whose work on the Appalachian/Caledonian Orogen, in our humble opinion the most beautiful and challenging orogen on our planet, was an inspiration to us all. The first author gratefully acknowledges the support of Geological Survey of Canada, Natural Science and Engineering Research Council, Ontario Graduate Scholarship Program and Strategic Areas of Development Program. The authors thank the Ottawa-Carleton Radiogenic Isotope Group and staff of Geological Survey of Canada geochronology laboratory for assisting in isotope analysis. This manuscript was significantly improved through the reviews of J. Kim, B. Murphy, A. Tremblay, J. Whalen, and R. Wintsch. This is Geological Survey of Canada contribution #20060079, TGI000018: Geology of the Iapetus Suture.

Appendix

SHRIMP II analyses were conducted at the Geological Survey of Canada (GSC) using analytical procedures described by Stern (1997), with standards and U-Pb calibration methods following Stern and Amelin (2003). Zircons from the samples were cast in 2.5 cm diameter epoxy mounts [GSC mount #257 for sample VLA01-067 (z7630) and GSC mount #295 for sample VLA01-314 (z7630)] along with fragments of the GSC laboratory standard zircon (z6266, with $^{206}Pb/^{238}U$ age = 559 Ma). The mid-sections of the zircons were exposed using 9, 6, and 1 μm diamond compound, and the internal features of the zircons were characterized with backscatter electrons (BSE) and cathodoluminescence (CL) utilizing a Cambridge Instruments scanning electron microscope (SEM). Mount surfaces were evaporatively coated with 10 nm of high purity Au. Analyses were conducted using an $^{16}O^-$ primary beam, projected onto the zircons at 10 kV. The sputtered area used for analysis was ca. 25 μm in diameter with a beam current of ca. 13 nA and 5 nA for z7252 and z7630, respectively. The count rates of ten isotopes of Zr^+, U^+, Th^+, and Pb^+ in zircon were sequentially measured over 6 scans (sample z7252) or 4 scans (z7630) with a single electron multiplier and a pulse counting system with deadtime of 35 ns. Off-line data processing was accomplished using customized in-house software. The 1σ external errors of $^{206}Pb/^{238}U$ ratios reported in table 1 incorporate a ±1.0 percent error in calibrating the standard zircon (see Stern and Amelin, 2003). No fractionation correction was applied to the Pb-isotope data; common Pb correction utilized the measured $^{204}Pb/^{206}Pb$ and compositions modeled after Cumming and Richards (1975). The $^{206}Pb/^{238}U$ ages for the analyses have been corrected for common Pb using both the 204- and 207-methods (Stern, 1997), but there is generally no significant difference in the results (table 1). Concordia ages (Ludwig, 1998) have been calculated for the samples presented in this paper. A Concordia age incorporates errors on the decay constants and includes both an evaluation of concordance and an evaluation of equivalence of the data (how well the data fit the assumption that they are repeated measurements of the same point). The calculated Concordia ages and errors quoted in the text are at 2σ with decay constant errors included.

References

Barker, D. H. N., Christeson, G. L., Austin, J. A., and Dalziel, I. W. D., 2003, Backarc basin evolution and Cordilleran orogenesis; insights from new ocean-bottom seismograph refraction profiling in Bransfield Strait, Antarctica: Boulder, Geology, v. 31, n. 2, p. 107–110.

Bedard, J. H., Lauziere, K., Tremblay, A., and Sangster, A., 1998, Evidence for forearc seafloor-spreading from the Betts Cove Ophiolite, Newfoundland; oceanic crust of boninitic affinity: Tectonophysics, v. 284, n. 3-4, p. 233–245.

Boone, G. M., Doty, D. T., and Heizler, M. T., 1989, Hurricane Mountain Formation melange; description and tectonic significance of a Penobscottian accretionary complex: Maine Geological Survey, Studies in Maine Geology, p. 33–83.

Bostock, H. H., 1988, Geology and petrochemistry of the Ordovician volcano-plutonic Robert's Arm Group, Notre Dame Bay, Newfoundland: Geological Survey of Canada, Geological Survey of Canada Bulletin 369, 84 p.

Cabanis, B., and Lecolle, M., 1989, Le diagramme La/10-Y/15-Nb/8; un outil pour la discrimination des series volcaniques et la mise en evidence des processus de melange et/ou de contamination crustale. The La/10-Y/15-Nb/8 diagram; a tool for distinguishing volcanic series and discovering crustal mixing and/or contamination: Comptes Rendus de l'Academie des Sciences, Serie 2, Mecanique, Physique, Chimie, Sciences de l'Univers: Sciences de la Terre, v. 309, n. 20, p. 2023–2029.

Cann, J. R., 1970, Rb, Sr, Y, Zr and Nb in some ocean floor basaltic rocks: Earth and Planetary Science Letters, v. 10, n. 1, p. 7–11.

Cloos, M., 1993, Lithospheric buoyancy and collisional orogenesis; subduction of oceanic plateaus, continental margins, island arcs, spreading ridges, and seamounts: Geological Society of America Bulletin, v. 105, n. 6, p. 715–737.

Colman-Sadd, S. P., Dunning, G. R., and Dec, T., 1992, Dunnage-Gander relationships and Ordovician orogeny in central Newfoundland; a sediment provenance and U/Pb age study: American Journal of Science, v. 292, n. 5, p. 317–355.

Cumming, G. L., and Richards, J. R., 1975, Ore lead in a continuously changing Earth: Earth and Planetary Science Letters, v. 28, p. 55–171.

D'Lemos, R. S., and Holdsworth, R. E., 1995, Samarium-neodymium isotopic characteristics of the northeastern Gander Zone, Newfoundland Appalachians: Special Paper - Geological Association of Canada, v. 41, p. 239–252.

Dalziel, I. W. D., 1986, Collision and Cordilleran orogenesis; an Andean perspective, *in* Coward, M. P., and Ries, A. C., editors, Collision Tectonics: London, Geological Society Special Publication, v. 19, p. 389–404.

Dunning, G. R., and Krogh, T. E., 1985, Geochronology of ophiolites of the Newfoundland Appalachians: Canadian Journal of Earth Sciences, v. 22, n. 11, p. 1659–1670.

Dunning, G. R., Kean, B. F., Thurlow, J. G., and Swinden, H. S., 1987, Geochronology of the Buchans, Roberts Arm, and Victoria Lake groups and Mansfield Cove Complex, Newfoundland: Canadian Journal of Earth Sciences, v. 24, n. 6, p. 1175–1184.

Dunning, G. R., Swinden, H. S., Kean, B. F., Evans, D. T. W., and Jenner, G. A., 1991, A Cambrian island arc in Iapetus; geochronology and geochemistry of the Lake Ambrose volcanic belt, Newfoundland Appalachians: Geological Magazine, v. 128, n. 1, p. 1–17.

Evans, D. T. W., and Kean, B. F., 2002, The Victoria Lake supergroup, central Newfoundland - its definition, setting and volcanogenic massive sulphide mineralization: Newfoundland Department of Mines and Energy, Geological Survey, Open File NFLD/2790, p. 68.

Evans, D. T. W., Kean, B. F., and Dunning, G. R., 1990, Geological studies, Victoria Lake Group, central Newfoundland: Newfoundland Department of Mines and Energy, Geological Survey, Report 90-1, p. 131–144.

Falloon, T. J., and Crawford, A. J., 1991, The petrogenesis of high-calcium boninite lavas dredged from the northern Tonga Ridge: Earth and Planetary Science Letters, v. 102, n. 3-4, p. 375–394.

Foerster, H. J., Tischendorf, G., and Trumbull, R. B., 1997, An evaluation of the Rb vs. (Y+Nb) discrimination diagram to infer tectonic setting of silicic igneous rocks: Lithos, v. 40, n. 2-4, p. 261–293.

Fryer, P., and Pearce, J. A., 1992, Introduction to the scientific results of Leg 125, *in* Fryer, P., Pearce, J. A., Stokking, L. B., Ali, J. R., Arculus, R., Ballotti, D. L., Burke, M. M., Ciampo, G., Haggerty, J. A., Haston, R. B., Heling, D., Hobart, M. A., Ishii, T., Johnson, L. E., Lagabrielle, Y., McCoy, F. W., Maekawa, H., Marlow, M. S., Milner, G. J., Mottl, M. J., Murton, B. J., Phipps, S. P., Rigsby, C. A., Saboda, K. L., Stabell, B., van der Laan, S., and Xu, Y., editors: Proceedings of the Ocean Drilling Program, Scientific Results, 125, p. 3–11.

Gamble, J. A., Wright, I. C., Woodhead, J. D., and McCulloch, M. T., 1995, Arc and back-arc geochemistry in the southern Kermadec arc - Ngatoro Basin and offshore Taupo Volcanic Zone, SW Pacific, *in* Smellie, J. L., editor, Volcanism associated with extension at consuming plate margins: London, Geological Society Special Publication, v. 81, p. 193–212.
Jacobi, R. D., and Wasowski, J. J., 1985, Geochemistry and plate-tectonic significance of the volcanic rocks of the Summerford Group, north-central Newfoundland: Boulder, Geology, v. 13, n. 2, p. 126–130.
Jenner, G. A., and Swinden, H. S., 1993, The Pipestone Pond Complex, central Newfoundland; complex magmatism in an eastern Dunnage Zone ophiolite: Canadian Journal of Earth Sciences, v. 30, n. 3, p. 434–448.
Johnson, S. C., and McLeod, M. J., 1996, The New River Belt; a unique segment along the western margin of the Avalon composite terrane, southern New Brunswick, Canada: Geological Society of America Special Paper, v. 304, p. 149–164.
Kay, M., 1967, Stratigraphy and structure of northeastern Newfoundland bearing on drift in North Atlantic: The American Association of Petroleum Geologists Bulletin, v. 51, n. 4, p. 579–600.
Kean, B. F., 1977, Geology of the Victoria Lake area (12-A/06), Newfoundland: Newfoundland and Labrador Department of Mines and Energy, Mineral Development Division, Report N. 77-4, 11 p.
——— 1983, King George IV Lake, Grand Falls district, Newfoundland, Map 82-051, scale 1:50,000, 1 sheet, Geology of the King George IV Lake map area (12-A/4): Government of Newfoundland and Labrador, Department of Mines and Energy, Mineral Development Division, p. 74.
Kean, B. F., and Jayasinghe, N. R., 1980, Badger, Grand Falls District, Newfoundland (12A/16): Government of Newfoundland and Labrador, Department of Mines and Energy, Mineral Development Division, Report 81–02.
——— 1981, Geology of the King George IV map area (12A/4), Newfoundland: Government of Newfoundland and Labrador, Department of Mines and Energy, Mineral Development Division, Report n. 81-1, p. 32–39.
Kean, B. F., and Mercer, N. L., 1981, Grand Falls, Newfoundland: Government of Newfoundland and Labrador, Department of Mines and Energy, Mineral Development Division, Map 81-099, Scale: 1:50 000.
Kerr, A., Jenner, G. A., and Fryer, B. J., 1995, Sm-Nd isotopic geochemistry of Precambrian to Paleozoic granitoid suites and the deep-crustal structure of the southeast margin of the Newfoundland Appalachians: Canadian Journal of Earth Sciences, v. 32, n. 2, p. 224–245.
Kimura, G., and Ludden, J., 1995, Peeling oceanic crust in subduction zones: Boulder, Geology, v. 23, n. 3, p. 217–220.
Lissenberg, C. J., Zagorevski, A., Rogers, N., van Staal, C. R., Whalen, J. B., and McNicoll, V., 2005, Geology, Star Lake, Newfoundland (NTS 12-A/11): Geological Survey of Canada Open File 1669, scale 1:150.000.
Ludwig, K. R., 1998, On the treatment of concordant uranium-lead ages: Geochimica et Cosmochimica Acta, v. 62, n. 4, p. 665–676.
——— 2001, User's manual for Isoplot/Ex rev. 2.49: a Geochronological Toolkit for Microsoft Excel: Berkeley, Berkeley Geochronology Center.
MacLachlan, K., and Dunning, G., 1998a, U-Pb ages and tectonomagmatic relationships of early Ordovician low-Ti tholeiites, boninites and related plutonic rocks in central Newfoundland, Canada: Contributions to Mineralogy and Petrology, v. 133, n. 3, p. 235–258.
MacLachlan, K., and Dunning, G. R., 1998b, U-Pb ages and tectonomagmatic relationships of Middle Ordovician volcanic rocks of the Wild Bight Group, Newfoundland Appalachians: Canadian Journal of Earth Sciences, v. 35, p. 998–1017.
MacLachlan, K., O'Brien, B. H., and Dunning, G. R., 2001, Redefinition of the Wild Bight Group, Newfoundland; implications for models of island-arc evolution in the Exploits Subzone: Canadian Journal of Earth Sciences, v. 38, n. 6, p. 889–907.
Macpherson, C. G., and Hall, R., 2001, Tectonic setting of Eocene boninite magmatism in the Izu-Bonin-Mariana forearc: Earth and Planetary Science Letters, v. 186, n. 2, p. 215–230.
McLeod, M. J., Johnson, S. C., and Krogh, T. E., 2003, Archived U-Pb (zircon) dates from southern New Brunswick: Atlantic Geology, v. 39, p. 209–225.
McNicoll, V., van Staal, C. R., and Waldron, J. W. F., 2001, Accretionary history of the northern Appalachians: SHRIMP study of Ordovician-Silurian syntectonic sediments in the Canadian Appalachians: Geological Society of America, Abstracts with Programs, v. 26, p. 100.
McNicoll, V. J., Whalen, J. B., and Stern, R. A., 2003, U-Pb geochronology of Ordovician plutonism, Bathurst mining camp, New Brunswick: Economic Geology Monographs, v. 11, p. 203–218.
Monzier, M., Danyushevsky, L. V., Crawford, A. J., Bellon, H., and Cotten, J., 1993, High-Mg andesites from the southern termination of the New Hebrides island arc (SW Pacific): Journal of Volcanology and Geothermal Research, v. 57, n. 3-4, p. 193–217.
Nelson, K. D., 1981, Melange development in the Boones Point Complex, North-central Newfoundland: Canadian Journal of Earth Sciences, v. 18, n. 3, p. 433–442.
O'Brien, B., Swinden, H. S., Dunning, G. R., Williams, S. H., and O'Brien, F. H. C., 1997, A peri-Gondwanan arc-back arc complex in Iapetus; Early-Mid Ordovician evolution of the Exploits Group, Newfoundland: American Journal of Science, v. 297, n. 2, p. 220–272.
O'Brien, B. H., 1992, Internal and external relationships of the South Lake igneous complex, north-central Newfoundland (NTS 2E/5, 6); Ordovician and later tectonism in the Exploits subzone: Current Research, Newfoundland Geological Survey Branch, Report: 92-1, p. 159–169.
Pearce, J. A., Harris, N. B. W., and Tindle, A. G., 1984, Trace element discrimination diagrams for the tectonic interpretation of granitic rocks: Journal of Petrology, v. 25, n. 4, p. 956–983.

Pollock, J. C., and Wilton, D. H. C., 2001, Metallogenic studies of the Tally Pond Belt, Victoria Lake Group; trace-element geochemistry and lead-isotope data from the Exploits Subzone, Newfoundland: Government of Newfoundland and Labrador Department of Mines and Energy, Geological Survey, Report 2001-1, p. 247–266.

Pollock, J. C., Wilton, D. H. C., and van Staal, C. R., 2002, Geological studies and definition of the Tally Pond Group, Victoria Lake Supergroup, Exploits Subzone, Newfoundland Appalachians: Current Research - Newfoundland Geological Survey Branch, Report: 02-1, p. 155–167.

Pollock, J., McNicoll, V., van Staal, C. R., Wilton, D., and Anonymous, 2004, Geology of the Tally Pond Group, Newfoundland; new geochronology and geochemical data from the Exploits Subzone, Dunnage Zone: Geological Society of America, Abstracts with Programs, v. 36, n. 2, p. 129.

Rogers, N., 2004, Red Indian Line geochemical database: Geological Survey of Canada Open File 4605.

Rogers, N., and van Staal, C. R., 2002, Toward a Victoria Lake Supergroup; a provisional stratigraphic revision of the Red Indian to Victoria lakes area, central Newfoundland: Current Research - Newfoundland Geological Survey Branch, Report: 02-1, p. 185–195.

——— 2003, Volcanology and tectonic setting of the northern Bathurst mining camp; Part II, Mafic volcanic constraints on back-arc opening: Economic Geology Monographs, v. 11, p. 181–201.

Rogers, N., van Staal, C. R., and Theriault, R., 2003, Volcanology and tectonic setting of the northern Bathurst mining camp; Part 1, Extension and rifting of the Popelogan Arc: Economic Geology Monographs, v. 11, p. 157–179.

Rogers, N., van Staal, C. R., and McNicoll, V., 2005a, Geology, Badger, Newfoundland (NTS 12-A/16), scale 1:50,000:Geological Survey of Canada, Open File 4546.

Rogers, N., van Staal, C. R., Pollock, J., and Zagorevski, A., 2005b, Geology, Lake Ambrose and part of Buchans, Newfoundland (NTS 12-A/10 and part of 12-A/15), scale 1:50,000.

Rogers, N., van Staal, C. R., McNicoll, V., Pollock, J., Zagorevski, A., and Whalen, J., 2006, Neoproterozoic and Cambrian arc magmatism along the eastern margin of the Victoria Lake Supergroup: a remnant of Ganderian basement in central Newfoundland?: Precambrian Research, v. 147, p. 320–341.

Şengor, A. M. C., and Natal'in, B. A., 1996, Turkic-type orogeny and its role in the making of the continental crust: Annual Review of Earth and Planetary Sciences, v. 24, p. 263–337.

Sobolev, A. V., and Danyushevsky, L. V., 1994, Petrology and geochemistry of boninites from the north termination of the Tonga Trench; constraints on the generation conditions of primary high-Ca boninite magmas: Journal of Petrology, v. 35, n. 5, p. 1183–1211.

Squires, G. C., and Moore, P. J., 2004, Volcanogenic massive sulphide environments of the Tally Pool Volcanics and adjacent area; geological, lithogeochemical and geochronological results: Newfoundland Department of Mines and Energy, Geological Survey, Current Research Report, 04-1, p. 63–91.

Stern, R. A., 1997, The GSC Sensitive High Resolution Ion Microprobe (SHRIMP); analytical techniques of zircon U-Th-Pb age determinations and performance evaluation: Geological Survey of Canada, Current Research, Report 1997-F, p. 1–31.

Stern, R. A., and Amelin, Y., 2003, Assessment of errors in SIMS zircon U–Pb geochronology using a natural zircon standard and NIST SRM 610 glass: Chemical Geology, v. 197, n. 1-4, p. 111–142.

Stern, R. J., and Bloomer, S. H., 1992, Subduction zone infancy; examples from the Eocene Izu–Bonin-Mariana and Jurassic California arcs: Geological Society of America Bulletin, v. 104, n. 12, p. 1621–1636.

Sun, S. S., and McDonough, W. F., 1989, Chemical and isotopic systematics of oceanic basalts; implications for mantle composition and processes, *in* Saunders, A. D., and Norry, M. J., editors, Magmatism in the Ocean Basins: London, Geological Society Special Publication, v. 42, p. 313–345.

Swinden, H. S., and Jenner, G. A., 1992, Volcanic stratigraphy northwest of New Bay Pond, central Newfoundland, and the strike-extent of the Point Leamington massive sulfide horizon: Newfoundland Geological Survey Branch, Current Research, Report: 92-1, p. 267–279.

Swinden, H. S., and Thorpe, R. I., 1984, Variations in style of volcanism and massive sulfide deposition in Early to Middle Ordovician island-arc sequences of the Newfoundland Central Mobile Belt: Economic Geology and the Bulletin of the Society of Economic Geologists, v. 79, n. 7, p. 1596–1619.

Swinden, H. S., Jenner, G. A., Fryer, B. J., Hertogen, J., and Roddick, J. C., 1990, Petrogenesis and paleotectonic history of the Wild Bight Group, and Ordovician rifted island arc in central Newfoundland: Contributions to Mineralogy and Petrology, v. 105, n. 2, p. 219–241.

Swinden, H. S., Jenner, G. A., and Szybinski, Z. A., 1997, Magmatic and tectonic evolution of the Cambrian-Ordovician Laurentian margin of Iapetus; geochemical and isotopic constraints from the Notre Dame Subzone, Newfoundland: Geological Society of America, Memoir, v. 191, p. 337–365.

Tucker, R. D., O'Brien, S. J., and O'Brien, B. H., 1994, Age and implications of Early Ordovician (Arenig) plutonism in the type area of the Bay du Nord Group, Dunnage Zone, southern Newfoundland Appalachians: Canadian Journal of Earth Sciences, v. 31, n. 2, p. 351–357.

Valverde-Vaquero, P., and van Staal, C. R., 2002, Geology and magnetic anomalies of the Exploits-Meelpaeg boundary zone in the Victoria Lake area (central Newfoundland); regional implications: Newfoundland Geological Survey Branch, Current Research, Report 02-1, p. 197–209.

Valverde-Vaquero, P., van Staal, C. R., McNicoll, V., and Dunning, G. R., 2006, Mid-Late Ordovician magmatism and metamorphism along the Gander margin in central Newfoundland: London, Journal of the Geological Society, v. 163, n. 2, p. 347–362.

van der Velden, A. J., van Staal, C. R., and Cook, F. A., 2004, Crustal structure, fossil subduction, and the tectonic evolution of the Newfoundland Appalachians; evidence from a reprocessed seismic reflection survey: Geological Society of America Bulletin, v. 116, n. 11-12, p. 1485–1498.

van Staal, C. R., 1994, Brunswick subduction complex in the Canadian Appalachians; record of the Late Ordovician to Late Silurian collision between Laurentia and the Gander margin of Avalon: Tectonics, v. 13, n. 4, p. 946–962.

van Staal, C. R., Winchester, J. A., and Bedard, J. H., 1991, Geochemical variations in Middle Ordovician volcanic rocks of the northern Miramichi Highlands and their tectonic significance: Canadian Journal of Earth Sciences, v. 28, n. 7, p. 1031–1049.

van Staal, C. R., Sullivan, R. W., and Whalen, J. B., 1996, Provenance of tectonic history of the Gander Zone in the Caledonian/Appalachian Orogen; implications for the origin and assembly of Avalon: Geological Society of America Special Paper, v. 304, p. 347–367.

van Staal, C. R., Dewey, J. F., Mac Niocaill, C., and McKerrow, W. S., 1998, The Cambrian-Silurian tectonic evolution of the Northern Appalachians and British Caledonides; history of a complex, west and southwest Pacific-type segment of Iapetus, *in* Blundell, D. J., and Scott, A. C., editors, Lyell: the Past is the Key to the Present: London, Geological Society Special Publication, v. 143, p. 199–242.

van Staal, C. R., Wilson, R. A., Rogers, N., Fyfee, L. R., Langton, J. P., McCutcheon, S. R., McNicoll, V., and Ravenhurst, C. E., 2003, Geology and tectonic history of the Bathurst Supergroup, Bathurst mining camp, and its relationships to coeval rocks in southwestern New Brunswick and adjacent mine; a synthesis, *in* Goodfellow, W. D., McCutrcheon, S. R., and Peter, J. M., editors, Massive sulfide deposits of the Bathurst Mining Camp, New Brunswick, and Northern Maine: Economic Geology Monograph 11, p. 37–60.

van Staal, C. R., Lissenberg, C. J., Pehrsson, S., Zagorevski, A., Valverde-Vaquero, P., Herd, R. K., McNicoll, V. J., and Whalen, J., 2005a, Geology, Puddle Pond, Newfoundland (NTS 12-A/05), scale 1:50,000.

van Staal, C. R., Valverde-Vaquero, P., Zagorevski, A., Boutsma, S., Pehrsson, S., van Noorden, M., and others, 2005b, Geology, King George IV Lake, Newfoundland (NTS 12-A/04), scale 1:50,000.

van Staal, C. R., Valverde-Vaquero, P., Zagorevski, A., Rogers, N., Lissenberg, C. J., and McNicoll, V., 2005c, Geology, Victoria Lake, Newfoundland (NTS 12-A/06), scale 1:50,000.

Whalen, J. B., Jenner, G. A., Longstaffe, F. J., Gariepy, C., and Fryer, B. J., 1997, Implications of granitoid geochemical and isotopic (Nd, O, Pb) data from the Cambrian-Ordovician Notre Dame Arc for the evolution of the Central Mobile Belt, Newfoundland Appalachians, *in* Sinha, A. K., Whalen, J. B., and Hogan, J., editors, The nature of magmatism in the Appalachian Orogen: Geological Society of America, Memoir, v. 191, p. 367–395.

Whalen, J. B., Rogers, N., van Staal, C. R., Longstaffe, F. J., Jenner, G. A., and Winchester, J. A., 1998, Geochemical and isotopic (Nd, O) data from Ordovician felsic plutonic and volcanic rocks of the Miramichi Highlands; petrogenetic and metallogenic implications for the Bathurst Mining Camp: Canadian Journal of Earth Sciences, v. 35, n. 3, p. 237–252.

Williams, H., 1995, Chapter 2: Temporal and spatial divisions, *in* Williams, H., editor, Geology of the Appalachian-Caledonian orogen in Canada and Greenland: Geological Survey of Canada, Geology of Canada, n. 6, p. 23–42.

Williams, H., Colman-Sadd, S. P., and Swinden, H. S., 1988, Tectonic-stratigraphic subdivisions of central Newfoundland: Geological Survey of Canada, Current Research, Part B, v. 88-1B, p. 91–98.

Williams, H., Currie, K. L., and Piasecki, M. A. J., 1993, The Dog Bay Line; a major Silurian tectonic boundary in Northeast Newfoundland: Canadian Journal of Earth Sciences, v. 30, n. 12, p. 2481–2494.

Williams, H., Lafrance, B., Dean, P. L., Williams, P. F., Pickering, K. T., and van der Pluijm, B. A., 1995, Chapter 4: Badger belt, *in* Williams, H., editor, Geology of the Appalachian - Caledonian orogen in Canada and Greenland: Geological Survey of Canada, Geology of Canada, n. 6, p. 403–413.

Winchester, J. A., and Floyd, P. A., 1977, Geochemical discrimination of different magma series and their differentiation products using immobile elements: Chemical Geology, v. 20, n. 4, p. 325–343.

Zagorevski, A., ms, 2006, Tectono-magmatic evolution of peri-Laurentian and peri-Gondwanan arc - backarc complexes along the Red Indian Line, central Newfoundland Appalachians: University of Ottawa, Ph. D. thesis, 309 p.

Zagorevski, A., Rogers, N., McNicoll, V., Lissenberg, C. J., van Staal, C. R., and Valverde-Vaquero, P., 2006, Lower to Middle Ordovician evolution of peri-Laurentian arc and back-arc complexes in the Iapetus: Constrains from the Annieopsquotch Accretionary Tract, central Newfoundland: Geological Society of America Bulletin, v. 118, n. 3/4, p. 324–342.